Proceedings World Geothermal Congress 2020+1
Reykjavik, Iceland, April - October 2021

Hydrogeochemistry of Chiweta Geothermal Prospect, Northern Malawi

Gift W. Tsokonombwe[a], Daði Þorbjörnsson[b], Sigurður G Kristinsson[b] Andri Stefánsson[c], Yankho Kalebe[d]

Department of Mining Engineering, Faculty of Engineering, The Polytechnic, University of Malawi P/Bag 303

Chichiri Blantyre 3, Malawi

[b] Iceland GeoSurvey (ISSOR) Grensasvegur 9, IS-108 Reykjavik, Iceland

[c] Institute of Earth Sciences, University of Iceland Sturlugata 7, IS-101 Reykjavík, Iceland

d Geological Survey Department (GSD), Regional Office Centre P.O. Box 30737 Lilongwe 3, Malawi

giftsokonombwe@gmail.com

Keywords: Geothermal, geochemistry, geothermometers

ABSTRACT

The geothermal and non-geothermal water chemistry associated with Chiweta geothermal prospect was studied. The main aim was to quantify chemical and physical characteristics of the geothermal water. Hydrogeological, geothermal mapping coupled with water chemistry was used to track water movement and quantification of related processes.

Thermal water hosted by metamorphic and Karroo sedimentary rocks emerge along NW-SE fault lineaments as hot springs, thermally altered grounds and shallow hot water borehole. Surface temperatures of thermal springs are about 80°C. The discharged thermal water from the 32 m depth well registered a temperature of 46°C.

The geothermal system of the Chiweta geothermal prospect is suggested to be a low temperature Neogene fault controlled geothermal system in the sedimentary environment. The recharge waters belong to Ca-Mg-HCO_3 type with a temperature between 23°C to 33°C and pH of 5.7-7.5. The inflow waters attain the heat from elevated geothermal gradient at depth, an anomaly assumed to be associated with crustal thinning due to Malawi Rift spreading. All thermal waters belong to Na-Cl-SO_4-HCO_3 facies. Chemical geothermometers suggest the subsurface reservoir temperature of about 132°C - 157°C. Multiple mineral equilibria and mixing models are in good agreement with the solute geothermometers estimated subsurface temperature range. The elevated temperature is enough to drive dissolution of host rock and ion exchange reaction in the reservoir of the geothermal system that modifies the chemical composition of the reservoir and thermal springs water to Na-Cl-SO_4-HCO_3 facies from recharged Ca-Mg-HCO_3 water type. The thermal water Cl/B ratio approached that of Cl/B rock ratio. No boiling is occurring during the ascent of the thermal waters but steaming at the surface causes minimal δD and $\delta^{18}O$ isotopic fractionation. Reservoir pH is slightly lower than in situ pH in the liquid phase due to loss of acid gases, mainly CO_2. Saturation of calcite and quartz is low in thermal spring waters indicating limited scaling potential. Reconstructed reservoir waters are saturated in talc, chrysotile, quartz and calcite indicating high chanced of scaling.

Both thermal and non-thermal waters of the Chiweta system originate as precipitation in the western highlands as indicated by δD and $\delta^{18}O$ stable isotopes. Heavily enriched δD and $\delta^{18}O$ isotope lake water do not contribute to recharge of the geothermal system.

1. INTRODUCTION

Geochemistry is used as an essential tool early stages of geothermal exploration as it can track back the origin of geothermal water and its flow direction. Waters and gases discharged at the surface generally carry imprints of their deeper processes such as fluid-rock interaction (Arnórsson, et al, 2007). As the primary fluid rises from deep apart of the system towards the surface it may go under phase separation due depressurisation boiling and result in formation of secondary fluid. In addition, secondary fluid is also formed when primary fluid mixes with surface waters (Arnórsson, et al, 2007). All these processes are captured in the chemistry of geothermal fluid discharged as geothermal manifestation. In addition, geothermal geochemistry aimed at studying water-rock interaction as dissolved constituents in the geothermal fluids as a product of fluid-rock interaction at depth and other processes (Arnórsson, et al, 2007).

Understanding of chemical processes within active geothermal systems has been advanced by thermodynamic and kinetic experiments and numerical modelling of fluid flow (Arnórsson et al., 2007). The chemical composition and isotope ratios of geothermal fluids provide important information about the geological, geochemistry and hydrogeological characteristics of geothermal systems. During exploitation geochemistry is used for monitoring reservoir response to utilization. With this background, Chiweta geothermal prospect was studied. The main focus is on the chemistry of the water recharging the geothermal system, reservoir fluid composition, water-rock interaction, and processes arising as hot water ascend to the surface.

Chiweta has the highest recorded temperature hot springs in Malawi, within a spring zone, sitting parallel to Mphinzi stream near the mouth of North Rumphi River, where temperature of 79°C is found. Few surrounding residences use the stream emanating from the springs for bathing and washing. A 32m deep shallow borehole drilled in March 2000 for cold water intercepted hot water that was used for bathing and washing. The borehole is located in the northeast of Chiweta hot springs, southeast of Luwuchi Primary School.

1.1 Location

Chiweta geothermal prospect is located in northern part of Rumphi District, northern region of Malawi between longitude 34.08°E and 34.21°E and latitude 10.62°S and 10.75°S (Figure 1). The prospect can be accessed through M1 road, about 120 km from Mzuzu City. The field is situated within few kilometres north of Chiweta trading centre. The site is comprised of Nyika escarpments belt of rugged country, consisting mainly of deeply dissected spurs which are almost V-shaped in the east and southwest. Elevation varies from 480 m at the shore of Lake Malawi to 1640 m above sea level at the crest of the escarpment. Flat areas are concentrated along the valleys and lake shore in the eastern side. The area experiences tropical climate with most of rains fall in the months of November to April and average annual rainfall of 1081 mm. Annual average atmospheric temperature is 24°C along the lake and 21° along the escarpment (Climate Data, 2017).

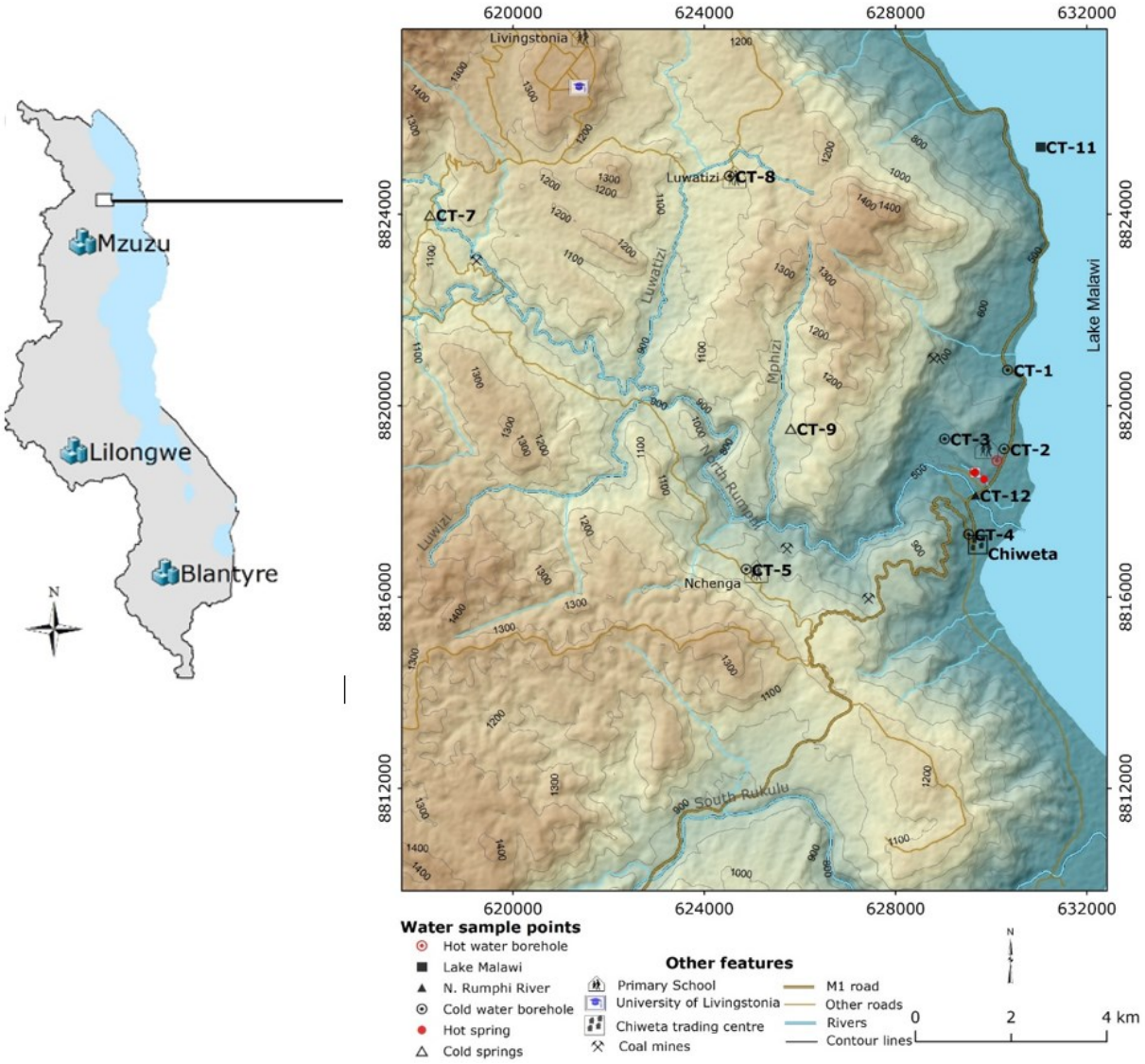

Figure 1: Map of Malawi showing location of study area and DEM Map showing the location of the Chiweta hot springs and water sampling points

1.2 Geology

The Geology of Livingstonia area in which the area under current study falls is mainly dominated by Karoo rocks, the unit that is found in Africa, Asia, Australia and South America and it correlate well in all these continents (Ring, 1995, Kemp, 1975, Thatcher, 1974). EARS Karoo graben is syn-depositional tectonic rifting related to incipient of break-up pattern of Gondwana connected to convective mantle. Lithostratigraphic nomenclature adopted for Karoo system ranges from K1 up to K7. Thatcher (1974) and Kemp (1975), summarise the geology of Uzumara South around Chiweta area. Units K1-K7 are displayed in Figure 2

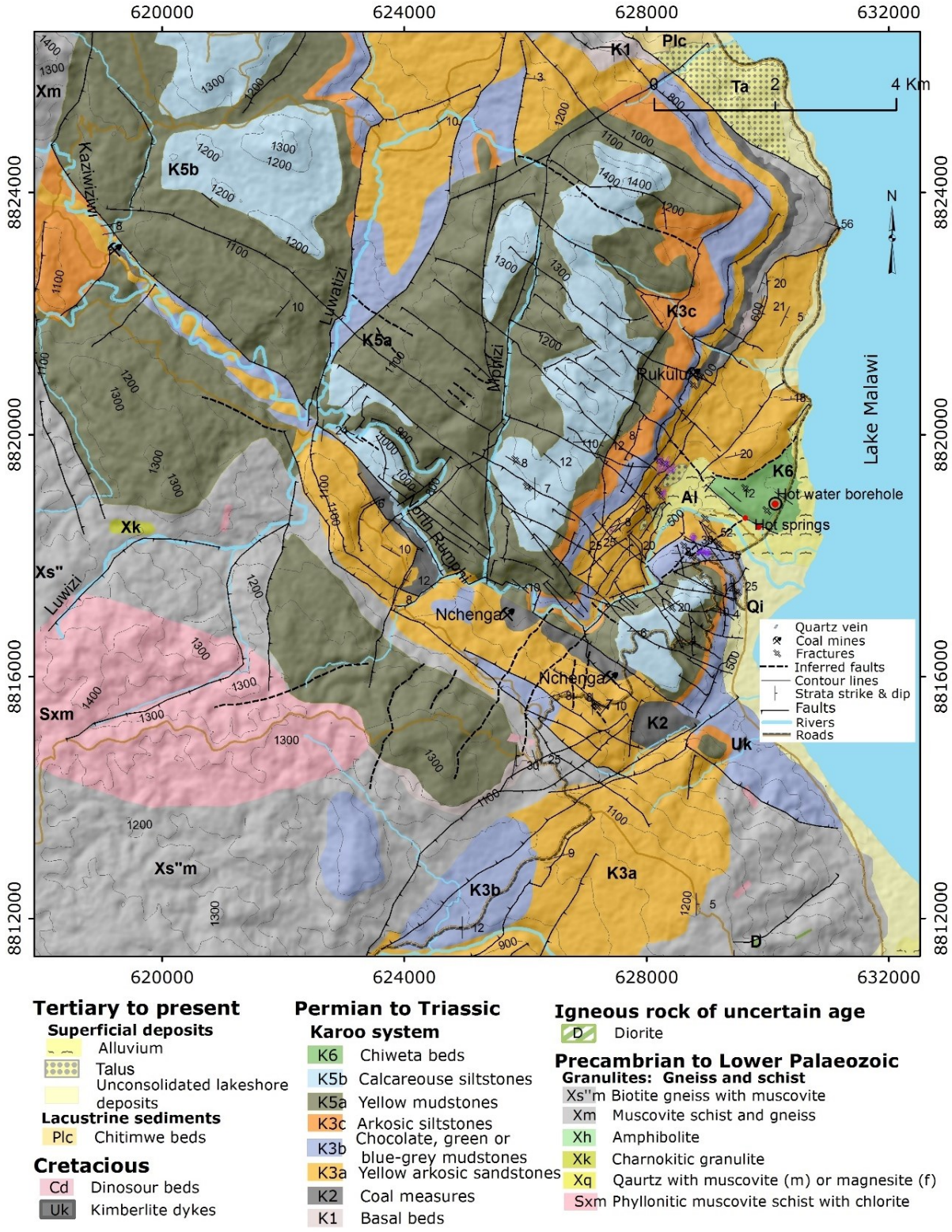

Figure 2: Structural and Geological map of Chiweta geothermal prospect. Based on Kemp (1975)

Structurally, Chiweta geothermal prospect rests within the Malawi Rift (Figure 3B), part of the western branch of the Cenozoic EARS (Figure 3A) which extends for about 800 km, from the Rungwe volcanics to southern Malawi. The rift structures extend for a further 600 km to the southern Africa via the Urema graben and Dombe trough in Mozambique. Malawi rift is classified as being in an initial-stage of rifting, characterized by divergences and subsidence along with frequent earthquakes (Chorowicz & Sorlien, 1992). The estimated relative spreading rate is about 2.2mm/year in the north and 1.5mm/yr in the south (Saria, Calais, Stamps, Delvaux, & Hartnady, 2014). It features less fault density and typified by extensional oblique-slip normal faulting basin. The basins are comprised of tens of km-long and 30-40 km wide box-like half-grabens, which at present are largely covered by Lake Malawi (Chorowicz and Sorlien, 1992). Initiation of rifting is estimated to be in late Miocene (Flannery and Rosendahl, 1990), or even earlier as oldest structures are estimated to be of Permian to Jurassic age (280-65 Ma) and linked to the orogenic episode associated with Karroo rifting (Mdala, 2015).

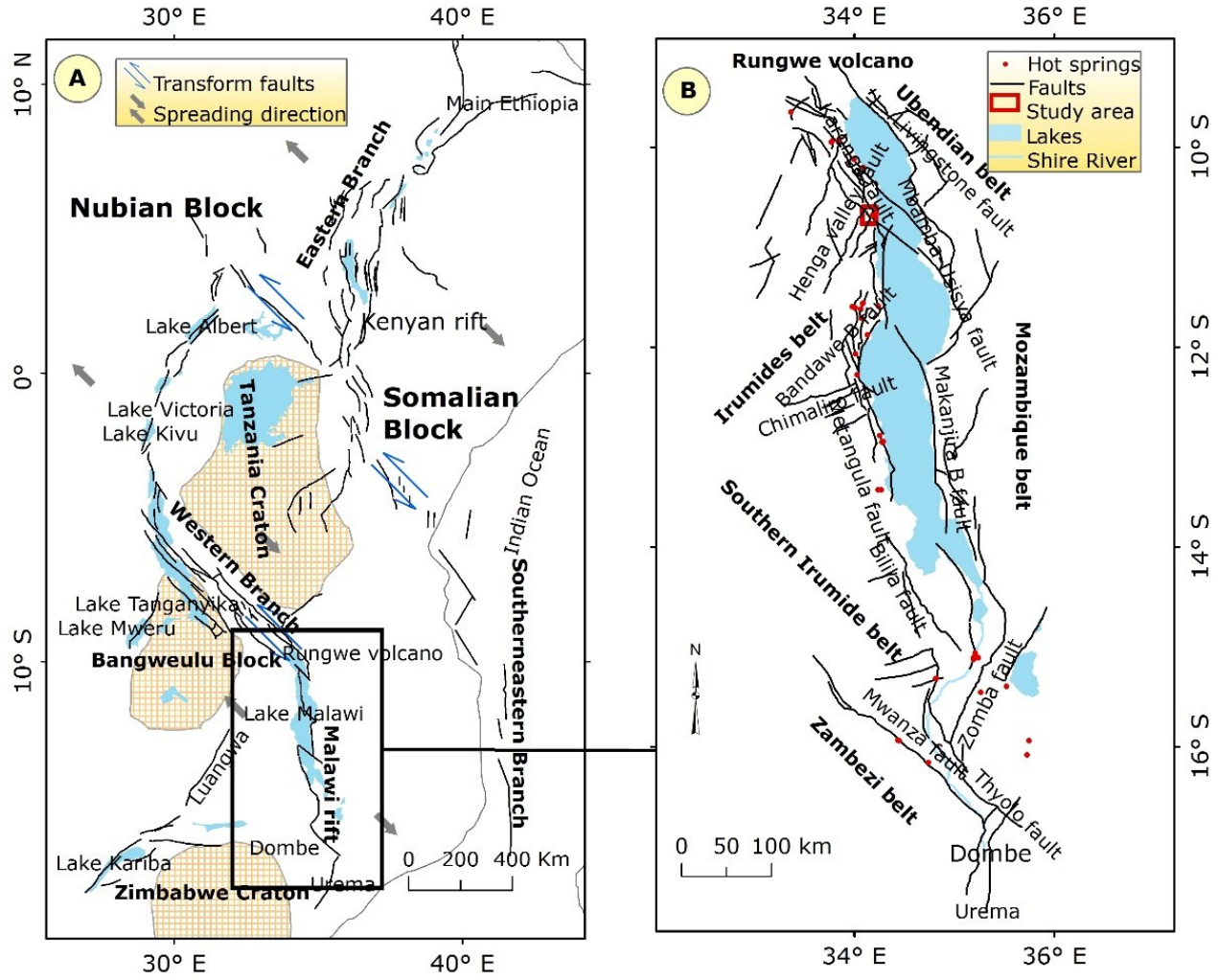

Figure 3. East Africa Rift System (A) showing Cratons, Rift branches, faults and plate motion (grey arrows) and Malawi rift in black box (B) showing major faults, mobile belts and Lungwe Valvano (Modified from Chorowicz, 2005)

1.3 Previous studies

Prior studies revealed that the thermal water of Chiweta are carbonate and sodium chloride type with fluorine content of 20 mg/kg (Kemp, 1975). Maximum temperature recorded at the surface was 78.3°C with total dissolved solids of 1198 mg/kg. The occurrence of hot springs has been interpreted as indicating presence of magmatism linked to the tectonic activity of EARS (Harrison and Chapusa, 1975) but a review of the available literature shows that main Malawi Rift has not been subjected to volcanic activity in recent times. The only known active volcanoes (erupted in the Holocene) (Fontijn et al., 2012) in the rift is located at Rungwe, Ngozi and Kyejo in the Rungwe Volcanic Province (RVP) in southwest Tanzania, about 280 km northeast of the Chiweta geothermal prospect. However, tectonism in Rungwe Volcanic Province affected northern part of Malawi rift (Dulanya et al., 2010).

Dulanya et al (2010) undertook a geothermometric study using silica (quartz and chalcedony) and cation (Na–K, Na–K–Ca and K–Mg) geothermometers to determine the subsurface temperatures of geothermal fields. This was achieved by using data published by Bloomfield & Garson, (1965), Harrison & Chapusa, (1975) and Ray (1975). Using methods proposed by Fournier (1973); Fournier and Truesdell (1973); and Truesdell A. H., & Fournier, (1977) they predicted subsurface temperature of 214°C at the Chinuka hot spring located at northern tip of Malawi (Dulanya et al., 2010).

Geochemical reconnaissance study by Geothermal Projects Limited of Malawi (Geothermal Development Company, 2010) estimated the subsurface temperatures of the Malawi geothermal systems using Na/K cation geothermometer of Fournier (1979) and Giggenbach (1988). Among hot springs studied, Chiweta springs registered the highest subsurface temperatures of 249°C.

Oklahoma State University and Geological Survey of Malawi collected thermal and non-thermal water samples around the country including the Chiweta in 2013 as part of investigation on the early stages of continental extension project. For comparison, the current study incorporated data collected by Oklahoma and Geothermal Projects Limited.

Wanda, Gulula, & Phiri, (2013) evaluated groundwater in entire the Rumphi area for irrigation suitability. Their study characterised the groundwater of the area as under-saturated with respect calcite and dolomite suggesting that a majority of the waters can allow dilution. High PCO_2 values were obtained in soil zones than in atmospheric suggesting that the groundwater system is enriched of soil CO_2. The groundwater is also saturated with respect to calcite and kaolinite stability field suggesting equilibrium of the

groundwater with respect to silicates. Their study concluded that chemical weathering and dissolution controls chemistry of groundwater of the area.

1.4 Objectives

None of studies carried out at Chiweta Geothermal Prospect narrate the geothermal activities of the area with respect to the origin of the geothermal water, sub-surface water rock interaction and modeling of water as it migrates from the reservoir till the surface. Therefore, the main aim of this study was to define the hydrogeological properties of thermal and non-thermal waters. Special emphasis was put on study of ground water movement from recharge zone to geothermal reservoir, modelling of reservoir fluid composition and water-rock interaction. To achieve these broad concepts the following objectives were set:

- To understand the basic hydrogeology of the study area in terms of the origin and movement of groundwater
- Estimate maximum subsurface reservoir temperature of the system by application of geothermometers and mixing models
- Validation of geothermometers using mixing models
- Reconstruct reservoir fluid composition
- Quantify various geochemical processes leading to the surface chemistry of hot water

2. METHODOLOGY

2.1 Water sampling, treatment and analysis

Sampling of water comprised of gathering information on chemical and physical characteristics on thermal and non-thermal water of the area. This involved collection of representative samples using sampling technics explained by Arnórsson et al., (2006) and Ármannsson & Ólafsson (2006). The hot water borehole was sampled as well. One sample was from North Rumphi River whereas the other one was from Lake Malawi. Two samples were collected from cold springs while the rest of the samples were from shallow drinking water boreholes.

In total twelve water samples were collected as shown in Figure 1 and Table 1. Samples were filtered on-site using cellulose acetate 0.2µm filter then each stored in a pair of polyethylene bottles. To prevent adsorption on the bottles wall, one of the bottles from the pair was acidified with 1 ml nitric acid (HNO_3) for determination of cations. The other sample was kept un-acidified for anion analyses. Temperature, electric conductivity (EC) and pH were measured directly during sample collection. The dissolved inorganic CO_2 was determined on-site using alkalinity titration where the sample was titrated from pH 8.4 using 0.1M of HCl to pH of 3.4. The concentration of CO_2 was determined using the following formula:

$$CO_2 = \left(\frac{ml\ HCl}{ml\ Sample}\right) \text{ x } 4400 - 6.76 \quad (1)$$

Dissolved H_2S was also determined onsite in thermal water samples by adding dithizone indicator into the sample, followed by titration with Hg acetate until the colour changed to pink. The amount of H_2S in the sample was derived using the following formula:

$$H_2S = \left(\frac{ml\ Mg\ acetate}{ml\ Sample}\right) \text{ x } 34 \quad (2)$$

The Cl and SO_4 were determined using Inductively Coupled Plasma Optical-Emission Spectrometry (ICP-OES) in un-acidified samples at the University of Iceland. Major cations such as Si, Na, K, Ca, Mg, Fe, Al and B were measured using the same ICP-OES on acidified sample. Florine and duplicate boron analysis was done using Ion Chromatography (IC-2000). For quality control of the analytical data, each sample was measured in duplicate and analysis of geothermal water standard was repeated at every 5 samples. The duplicate analytical precision at 95 % confidence level was less than 5 % for all measured elements. The stable isotopes of hydrogen (δD) and oxygen ($\delta^{18}O$) were analysed with an Inductively Coupled Plasma - Mass Spectrometer (ICP-MS).

Additional unpublished analytical data of Chiweta waters by Oklahoma State University and Geothermal Development Company (2010) were also included in this study.

Geochemical calculations including geothermometry, mineral saturation state, and reservoir composition of major elements were carried out with the aid of the WATCH (Bjarnason, 2010) and methods explained by Arnórsson et al., 2007 and D'Amore & Arnórsson (2000). Mixing models and stable isotope calculation were done using methods proposed by Arnórsson (2000 and Fournier & Potter (1982). .3. RESULTS

3.1 Geothermal mapping

The Chiweta geothermal prospect has near to boiling hot springs. Figure 4 (A&B), displays Chiweta springs oozing within N 310° W striking fault. The flow of hot water was about 30 L/s with most of the water coming from springs of temperature range between 60 and 80°C. Traces of sulphur and silica were noted deposited around springs and hot grounds area. The hot spring area also smells sulphur. Shallow water borehole drilled on Chiweta beds about 450 m northeast of the springs (Figure 1) close to Luwichi Primary School strike 46 °C hot water at a depth of 32 m.

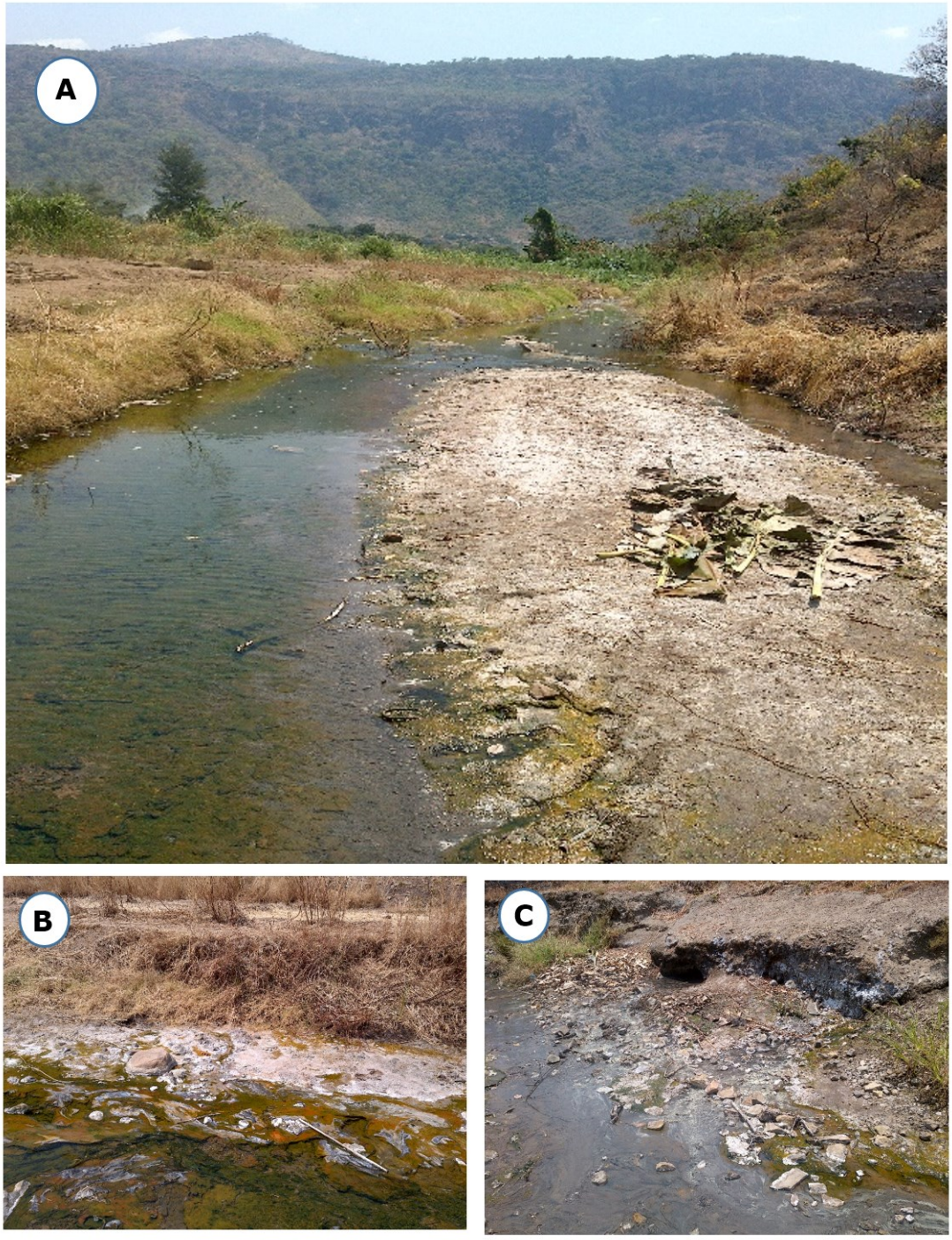

Figure 4: Chiweta hot springs flow (A), thermal altered surfaces along hot spring area (B) and thermal spring oozing from bottom of exposed Chiweta Beds(C). The actual location is shown in Figure 1 Error! Reference source not found.

3.2 Water chemistry

The results of the chemical analysis from Chiweta hot springs, boreholes, North Rumphi River and Lake Malawi waters are presented in Table 1. The table also include analytical data from the previous investigations by Oklahoma State University of USA (sample: CH-13, LM-13 and NR-13) and Geothermal Development Company (GDC) of Kenya (sample: CH-10 and LM-10) (Geothermal Development Company, 2010).

3.2.1 Surface water

Temperature of North Rumphi River (CT-12 and NR-13) and Lake Malawi waters (CT-11 and LM-13) were close to ambient 16 to 27°C. The electric conductivity (EC) ranged from 29 to 250 µS/cm. The dominant anion was bicarbonate. The pH of the lake and the river were neutral to slightly basic (7.6-8.8). The dominant cations in the Lake water were Ca and Na whereas Si and Ca dominate in the river water. Boron concentration of the waters was very minimal (<0.068 ppm).

3.2.2 Groundwater

For the cold groundwater (CT-2, CT-3, CT-4, CT-7 and CT-9), temperatures between 23 and 33°C was obtained with EC between 85 and 726 µS/cm. The pH varied from slightly acidic to neutral (5.7-7.5). Silica concentration was relatively medium ranging from 32 to 54 ppm whereas boron was very minimal. HCO_3 was dominant anion typically with concentration between 60- 220 ppm while Na and Si were dominant cations. Concentrations of many metals were low including Al and Fe whereas Mg was relatively high. The mild acidic pH groundwater was characterised with high CO_2 as well as slightly elevated Ca concentration.

3.2.3 Geothermal water

Geothermal water had higher EC ranging from 1771 to 2000 µS/cm. The surface temperature of thermal water registered minimum and maximum temperature of 60 and 79°C respectively with neutral pH of 7.8. The concentration of SiO_2 were relatively higher ranging from 31 to 99 ppm with sample CT-6 recorded the highest and the borehole water sample (CT-10) registered 72.83 ppm. The governing cations were Si and Na whereas leading anions were Cl and SO_4. Hot spring water registered low concentration in metals except for Mg which was slightly high in thermal water from the borehole.

Table 1. Chemical analysis of major elements determined by ICP-EOS and IC 2000. Isotopes were measured using ICP-MS. Temperature, pH, EC, CO_2 and H_2S were measured in the field with portable instruments. Concentrations of all chemical components are shown in ppm and isotopes in ‰.

Sample Name	Description	T (°C)	pH	pH/°C	Ec(µS)	SiO_2	Na	K	Ca	Mg	Fe	Al	B	$SO4^{2-}$	F^-	Cl^-	CO_2	H_2S	Dδ	$\delta^{18}O$
CT-1	Borehole	31	6	30.5	139.0	29.77	5.012	7.184	26.38	2.145	0.0488	0.0149	< 0.01	2.062	0.410	1.554	71.5	n.a.	-26.10	-4.90
CT-2	Borehole	33	7	30.9	500.0	39.77	40.59	2.969	47.36	13.31	0.0429	< 0.0075	0.0167	27.89	1.149	5.233	165	n.a.	-18.78	-3.07
CT-3	Borehole	27	6.59	35.9	246.0	27.91	8.642	5.012	17.82	6.182	7.734	0.0158	0.0331	1.069	0.701	3.671	60.1	n.a.	-22.20	-3.96
CT-4	Borehole	30	6.80	30.8	726.0	44.85	26.42	1.398	47.85	24.30	0.223	< 0.0075	< 0.01	17.26	0.645	1.614	220	n.a.	-23.66	-4.38
CT-5	Borehole	27.0	6.80	30.2	505.0	31.02	27.49	2.754	46.61	20.42	0.104	< 0.0075	< 0.01	6.426	0.740	3.319	155	n.a.	-27.25	-4.96
CT-8	Borehole	24	5.80	25.5	91.0	53.92	10.77	2.911	9.508	2.035	0.0190	< 0.0075	< 0.01	1.134	0.059	0.730	77.7	n.a.	-29.01	-5.21
CT-10	Borehole	46	7.5	39.5	1771.0	72.83	287.6	18.44	43.82	8.277	0.4035	< 0.0075	0.4924	245.8	8.846	230.8	106	0.230	-19.19	-3.56
CT-6	Hot spring	78.0	7.80	38.4	1900.0	99.43	383.0	23.20	17.96	0.387	< 0.005	0.0114	0.6954	295.7	12.63	336.7	59.3	2.02	-23.77	-4.08
CH-13[a]	Hot spring	80	7.5	35	2001	65.8	389.2	21.30	17.23	0.419	n.a.	n.a.	n.a.	287.3	12.82	316	28.0	n.a.	-26.0	-4.96
CH-10[b]	Hot spring	79.3	7.78	30.0	1 994	31.0	183.3	22.4	146.4	14.70	0.110	n.a.	n.a.	207	1.18	283.8	226	n.a.	n.a.	n.a.
CT-7	Cold spring	23.0	5.70	27.6	85.0	52.85	8.727	2.815	7.516	4.273	0.0175	< 0.0075	< 0.01	0.500	0.216	0.884	59.3	n.a.	-30.61	-5.24
CT-9	Cold spring	28	7.5	34.6	460.0	32.41	9.360	2.052	46.99	17.55	< 0.005	< 0.0075	< 0.01	12.09	0.531	1.759	122	n.a.	-23.00	-4.48
CT-11	L. Malawi	26	8.20	27.3	251.0	0.571	20.96	6.376	19.13	7.430	< 0.005	0.0105	0.0117	2.208	0.476	5.266	49.5	n.a.	15.06	2.27
LM-13[a]	L. Malawi	25.7	8.76	25.7	240	n.d.	20.04	6.01	17.53	6.89	n.a.	n.a.	n.a.	1.44	0.452	5.13	22.7	n.a.	12.49	1.67
LM-10[b]	L. Malawi	18.0	7.68	23.6	248	22.00	16.70	6.20	23.00	4.90	0.030	n.a.	n.a.	3.57	0.75	9.70	107	n.a.	n.a.	n.a.
CT-12	N. Rumphi River	22	7.6	22.3	29.6	13.81	2.078	1.141	3.021	1.117	0.0670	0.0229	< 0.01	1.218	0.059	0.737	2.19	n.a.	-34.01	-5.78
NR-13[a]	N. Rumphi River	16.5	8.3	17.0	31.0	9.270	2.220	0.909	2.72	0.992	n.a.	n.a.	n.a.	1.390	0.095	0.317	2.43	n.a.	-33.94	-6.50
Analytical uncertainties at 95% confidence level (unit %)						2.3	4.1	2.2	1.4	1.7	2.4	3.4	2.1	4.3	23.1	3.3	34.2	0.9		0.6
Detection limit (ppm)						0.1	0.25	0.4	0.025	0.005	0.005	0.0075	0.01	0.2	<0.1	1.0				

EC: electric conductivity

n.a.: not analysed, n.d.: not detected

[a] Oklahoma & GSD (2013), [b] GDC & GSD (2010)

3.2.4 Water classification

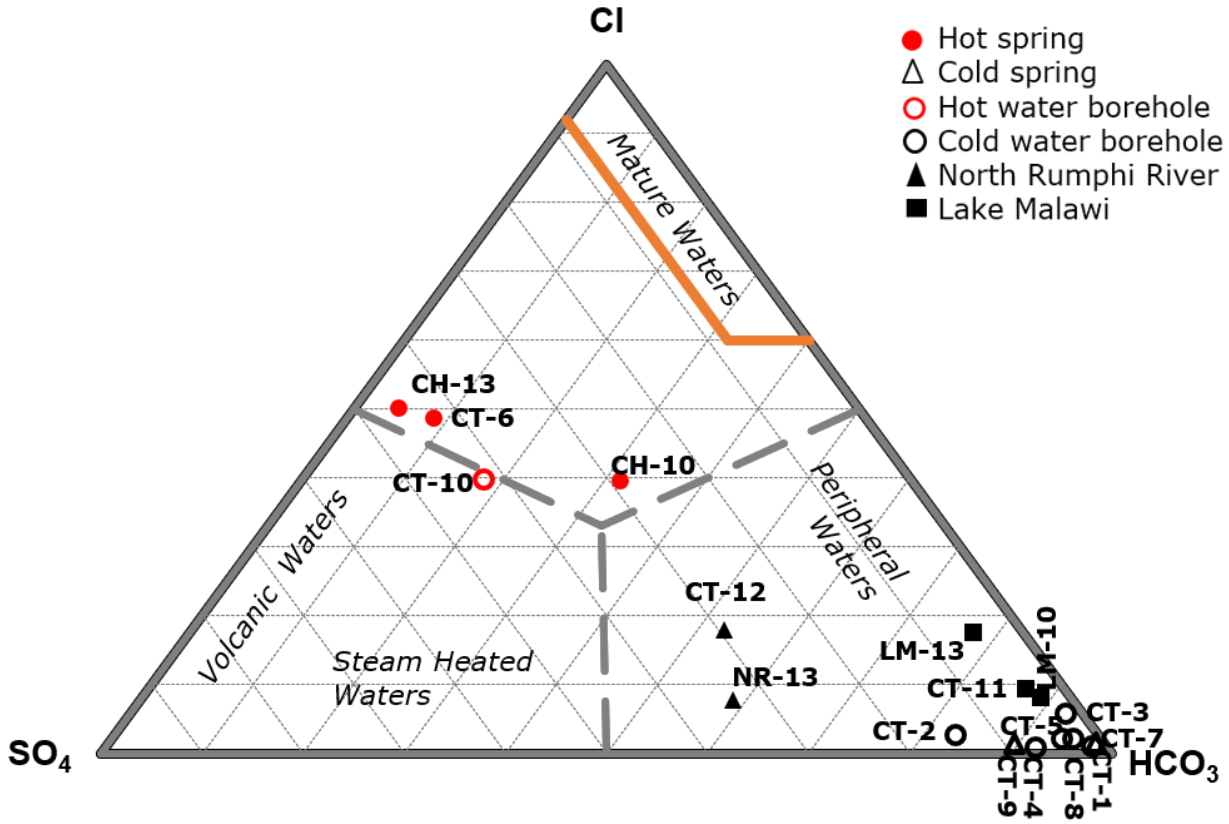

Figure 5. Cl-SO4-HCO3 water classification ternary diagram (Giggenbach, 1991) showing investigated water samples of Chiweta. Samples CH-13, NR-13 and ML-13 collected by Oklahoma State University in 2013. Samples CH-10 and ML-10 by GDC in 2010.

A triangular diagram of Giggenbach (1991) in Figure 5 displays cold groundwater and surface waters (samples; CT-1, CT-2, CT-3, CT-4, CT-5, CT-8, CT-9, CT-11, CT-12, ML-10, ML-13 and NR-13,) of Chiweta plotted in the peripheral water field of HCO_3 (bicarbonate). The geothermal water samples CT-6, CH-10, and CH-13 plotted in alkaline sulphate-chloride water region showing high input of geothermal water originating from controlled reactions dependent on temperature, pressure and rock composition of the subsurface. Therefore, these samples were useful in prediction of subsurface processes. Thermal water (CT-10) from the borehole plotted in steam heated field showing SO_4 component. The hot water from the borehole plotted sulphate water region suggesting oxidation of H_2S to SO_4 with most components dissolved from near surface rock. In such cases, this thermal water CT-10 does not fully represents subsurface properties as it indicates near surface processes. Therefore, use of such data in explaining subsurface processes was handled with cation. The cold groundwater from borehole, cold springs, North Rumphi River and Lake Malawi plotted in bicarbonate field representing peripheral waters as such they cannot used to explain any subsurface geothermal processes. In general, cold waters were not useful in identification of any subsurface geothermal processes. Figure 5 illustrated that the geothermal waters of Chiweta are Na-Cl-SO_4-HCO_3 (alkaline chloride) whereas the groundwater and surface water are Ca-Mg-HCO_3 (bicarbonate) water type.

3.3 Geothermometry

Figure 6 shows investigated samples plotted in Na-K-$Mg^{0.5}$ triangular diagram of (Giggenbach, 1988). Chiweta hot spring samples CT-6 and CH-13 plotted in partially equilibrated region implying that low Mg content reflected deeper water-mineral equilibration at high temperatures, followed by minor equilibration and uptake of Mg during ascent and discharge. In the same triangular plot in Figure 6 geothermal waters sampled from the borehole (CT-10) and hot spring (CH-10) plotted in immature water section suggesting more mixing and re-equilibration with near surface water such that they cannot be used to estimate subsurface temperature or else their geothermometry should be treated with caution.

3.3.1 Solute geothermometers

Table 2 shows solute geothermometers for the Chiweta geothermal prospect calculated from hot spring data in Table 1 using Powell & Cumming (2010) excel calculator, Bjarnason (2010) WATCH program and geothermometry equations reported by D'Amore & Arnórsson (2000). The calculated silica geothermometer of Fournier (1977) based chalcedony equilibration equation gave temperature range of 47 - 107°C for all samples. Field observation showed occurrence of hydrothermal quartz as opposite to chalcedony or amorphous silica meaning that eroded part of the hydrothermal alteration was at equilibrium with respect to quartz. Therefore, chalcedony geothermometer cannot give representative temperature despite sample CT-6 reservoir temperature of 107°C falls within chalcedony geothermometer applicable range. Silica and cation geothermometers (Arnorsson et al., 1983; Fournier, 1977; Fournier & Potter, 1982; Fournier & Truesdell, 1973; Truesdell, 1975) for samples CT-10, CH-13 and CH-10 gave a wide range of temperatures from 48 to 391°C. Such wide variation cannot be entrusted as subsurface temperature. Quartz geothermometer

conductive cooling by Fournier (1977) and adiabatic cooling gave reservoir temperature of 137 and 132°C respectively for sample CT-6. Fournier & Potter (1982) quartz geothermometer gave temperature of 134°C for the same sample. Truesdell (1975) and Arnorsson et al., (1983), Na-K geothermometers gave subsurface temperature of 139 and 149°C respectively for the same sample CT-6 again. The Na-K-Ca geothermometer of Fournier & Truesdell (973) indicated subsurface temperature of 157°C. The Na-K and Na-K-Ca geothermometers gave slightly higher temperatures than quartz geothermometer. The slight differences among cation and silica geothermometers in sample CT-6 indicate existence of equilibrium.

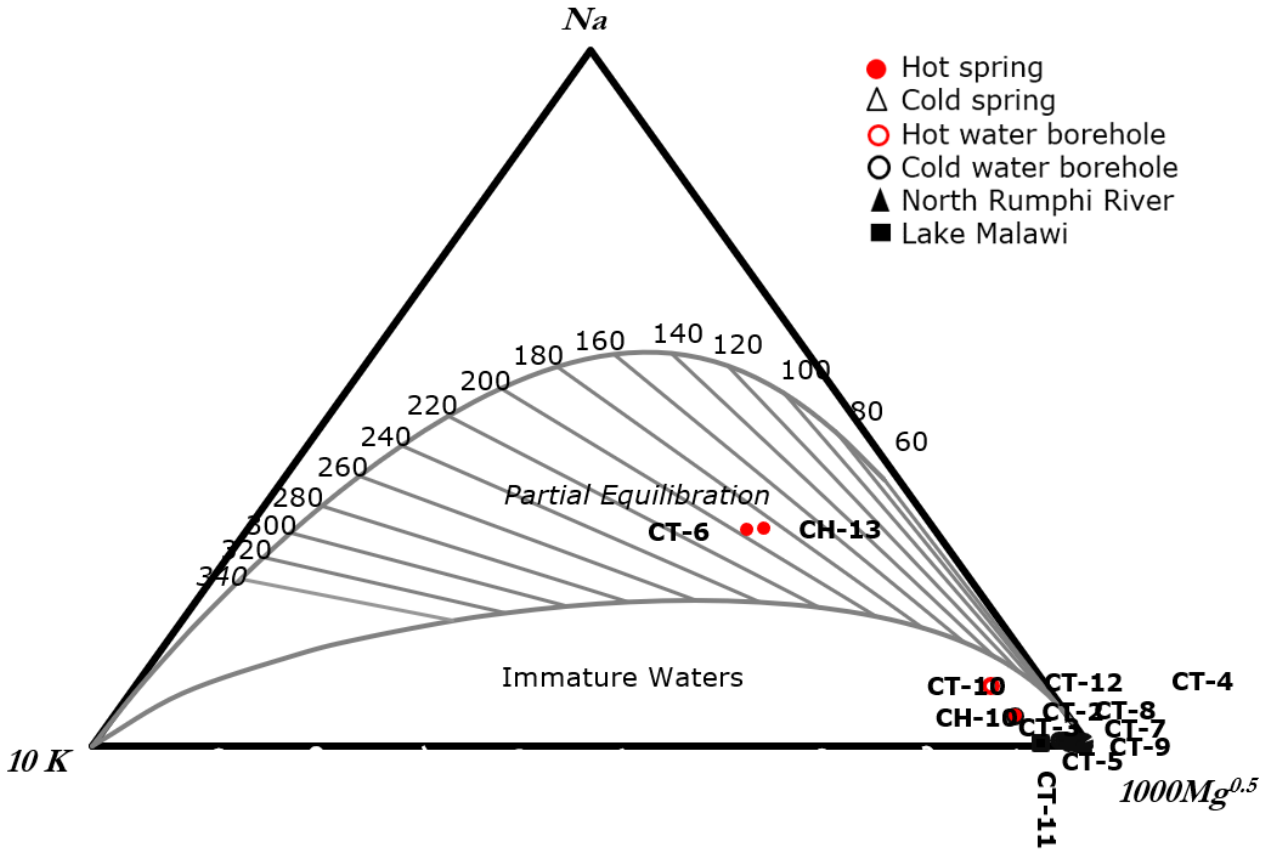

Figure 6. Na-K-Mg$^{0.5}$ triangular diagram (Giggenbach, 1988) of Chiweta thermal water samples. The current study sample (CT-6) and Oklahoma State University sample (CH-13) plotted in partial equilibrium region. Borehole sample from current study (CT-10) and spring sample collected by GDC (CH-10) plotted in immature field

All unitary geothermometers are prone to dilution such that low temperatures given by quartz and chalcedony geothermometers might be induced by dilution of geothermal water due to mixing with groundwater. On the other hand, Na-K cation geothermometer is least affected by dilution and conductive cooling where the flow rate is high. Therefore Na-K and Na-K-Ca geothermometers calculated above can be trusted considering that Chiweta springs flowrate is high (30 l/sec), the condition that qualify it to be least affected by conductive cooling. Therefore, the cation and silica geothermometers indicates true subsurface temperature represented by these geothermometers. However, both quartz and Na-K geothermometers gave temperature below their applicable range of > 150 and 180°C respectively. As stated earlier, field observations identified hydrothermal quartz, a signature of quartz equilibration on the eroded surface. Na-K can also predict low temperature geothermal system with long resident time water (D'Amore & Arnórsson, 2000). Sample CT-6 of Chiweta geothermal waters have high concentration of calcium such that log($Ca^{0.5}$/Na)+2.06 was positive (2.071) Therefore use of Na-K-Ca geothermometer was applicable (Fournier & Truesdell, 1973). As such, quartz, Na-K and Na-K-Ca geothermometer were suggested be true representative of the reservoir temperature. Based on sample CT-6 Chiweta geothermal system was therefore suggested to have subsurface temperature ranges between 132 and 157°C controlled by either quartz solubility or last equilibrated by Na-K and Na-K-Ca.

Table 2. Solute geothermometers for the Chiweta thermal spring water samples (values in °C)

Sample	Chalcedony [a]	Quartz [a]	Quartz [a]	Quartz [b]	Na/K [c]	Na/K [d]	Na-K-Ca [e]
CT-6	107	137	132	134	139	149	157
CT-10	90	120	118	119	144	156	116
CH-13	85	81	72	114	391	140	61
CH-10	48	67	84	80	210	223	88
Equation	3	4	5		7	8	9

[a](Fournier, 1977)
[b] (Fournier & Potter, 1982)
[c] (Truesdell, 1975)
[d] (Arnorsson et al., 1983)
[e] (Fournier & Truesdell, 1973)

3.3.2 Multiple mineral equilibria

Different approach of estimating subsurface temperature in geothermal system is calculation of reaction quotient Q (ionic activity product) and mass action K (equilibrium constant) of different species from analytical data of the hot springs, the method proposed by Reed & Spycher (1984). K is linked to Gibbs energy of reaction in the following equation:

$$\Delta_r G = -RTinK \quad (3)$$

Where $\Delta_r G$ Gibbs energy of reaction, R is gas constant, T represent temperature in kelvin and K is equilibrium constant.

Multiple mineral equilibria assume that temperature equilibrium exist between solute and minerals or mineral-mineral within which a set of minerals occur over a range of temperature. The equilibrium state of mineral such as silica (mainly quartz and chalcedony), sulfate (mainly gypsum and anhydrite) and carbonate (mainly calcite, aragonite, dolomite, siderite and magnesite) is the function of temperature, such that the saturation indices are used as geothermometer (Arnórsson, 2000; Giggenbach, 1988). The solute mineral equilibria temperature is a range or cluster between minimum and maximum equilibrium temperature for selected minerals over which most of the minerals appear to attain equilibrium. Where many minerals indicate close equilibrium temperatures, the average of equilibrium temperatures for a set of minerals is regarded as best subsurface temperature estimate. Apart from subsurface temperature estimation, saturation indices also entails possible problems such as calcite deposition and silica scaling that can arise due geothermal utilization.

Using mineral equilibria criteria, the geothermometry of Chiweta geothermal prospect was evaluated by calculating saturation indices of different minerals using WATCH software (Bjarnason, 2010). In general, multiple mineral equilibria shows calculated reservoir temperatures varying between 130 and 140°C which is in the same range with temperature calculated using quartz and Na-K geothermometers in Table 2.

The reservoir water showed highly saturated with respect to talc and chrysotile at temperatures lower than 140°C and slightly saturated with respect to calcite, quartz and microcline. These minerals were likely to form below that temperature. In hot spring water (sample CT-6) showed that most of the minerals including calcite, anhydrite, adularia, prehnite and muscovite were at disequilibrium. Similarly in discharged thermal water (CH-13) was at disequilibrium with respect to chalcedony and anhydrite. Both sample CT-6 and CHI-13 demonstrated that the hot spring waters were supersaturated with respect to calcite below 160°C and 130°C respectively. This mean calcite is likely to form below these temperatures. The result shows under saturation of chalcedony in hot spring waters from the aquafer temperature to discharging temperature substantiating that its geothermometer could not be reliable.

The disequilibrium conditions obtained in thermal spring and recalculated reservoir waters may be explained by mixing of thermal water with shallow waters.

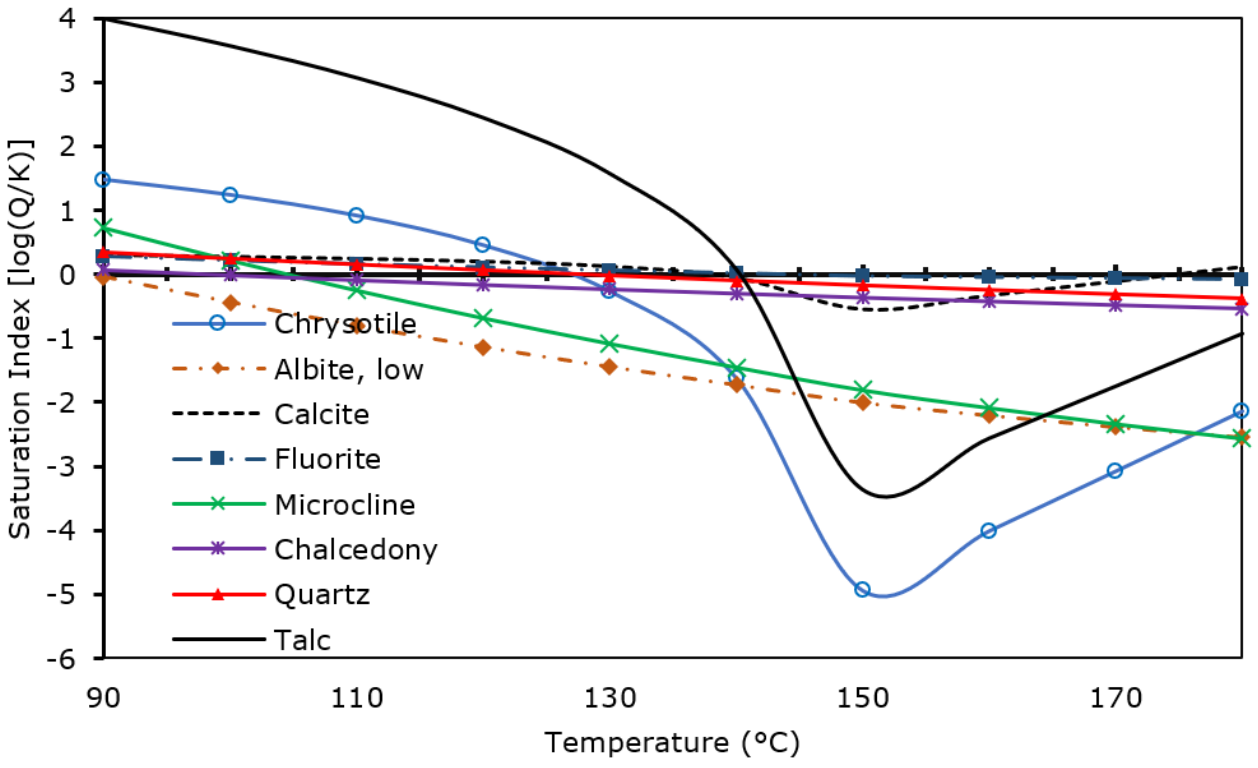

Figure 7. Saturation state of Chiweta geothermal aquifer water (based on sample CT-6) with respect to selected hydrothermal minerals as indicated. Equilibrium prevail within narrow range (130-140°C) indicating equilibrium conditions.

3.4 Mixing models

Chemical geothermometers estimate subsurface temperature from surface outflow composition with the notion that water cool in up-flow zone by either conductive cooling or adiabatically or both. Nevertheless, thermal water also cools through mixing with shallow cold groundwater. Cold groundwater are lower in dissolved solid such that mixing act as dilution to geothermal water (Arnórsson, 2000) that lead to erroneous geothermometer estimation. The application of mixing model to estimate subsurface temperature in geothermal system has demonstrated that mixture of two components of different composition can maintain composition of reactive component such that the concentration cannot change much after mixing has occurred in the upflow zone. Mixing models allows estimation of hot water component in the mixed waters emerging in spring or shallow drillhole. In the current study, three types of mixing models namely, silica-carbonate, silica-enthalpy and chloride-enthalpy mixing models (Arnórsson, 2000) were used.

3.4.1 The silica-carbonate model

The silica-carbonate model is based on the relationship between silica and carbonate and assumes that all silica exist in geothermal system as H_4SiO_4 and all carbonate as CO_2. The model assumes that both aqueous silica and total CO_2 concentrations are fixed by temperature dependent solute-mineral equilibrium in the reservoir whereas temperature dependence of silica is controlled by quartz. This model estimate the temperature of the hot water component and differentiate boiled geothermal water from non-boiled. The model curve in Figure 8 was created from SiO_2 and CO_2 concentration using the method described by Arnórsson (2000) and Fournier & Potter (1982).

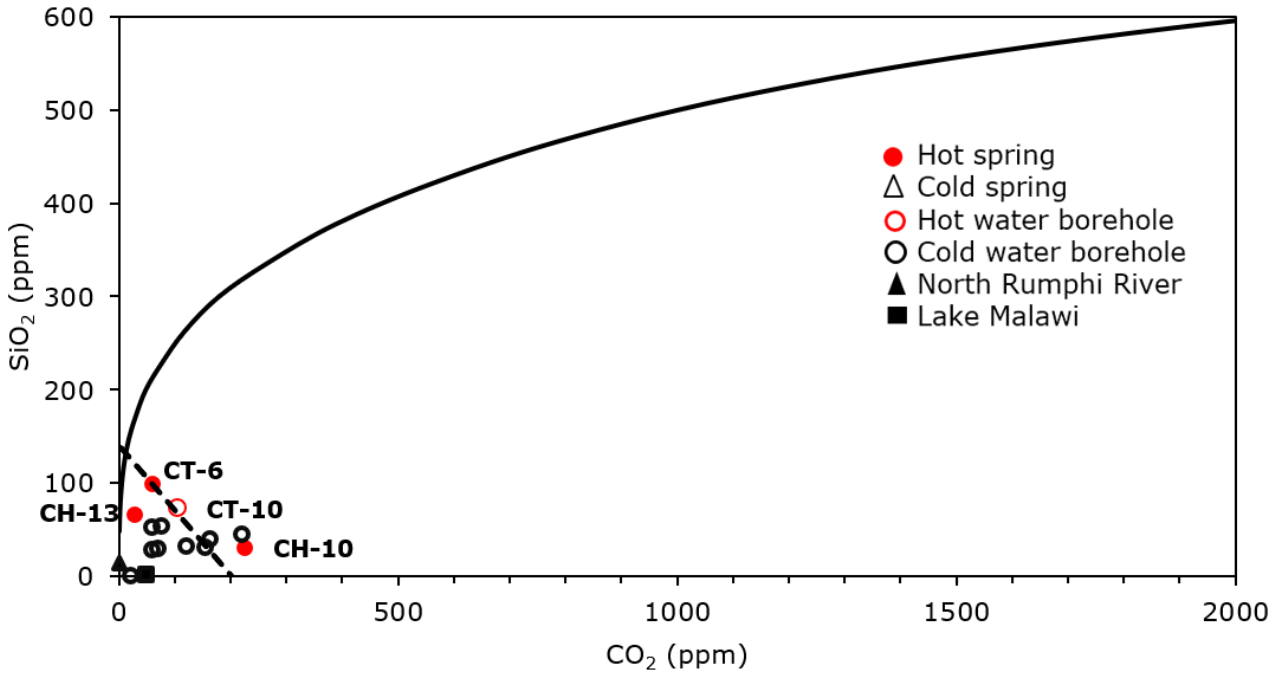

Figure 8. Silica-carbonate mixing model (Arnórsson, 2000) for thermal springs and non-thermal water at Chiweta. The intersection of dotted line and model curve gives the silica and carbonate concentration in hot water component. Silica is about 140 ppm.

Hot spring data points plotted below the curve indicating that hot spring waters were un-boiled. The intersection of an extrapolated line (from cold to mixed thermal water) with the model curve represents silica and carbonate concentration in the hot water component. The silica-carbonate model in Figure 8 demonstrates that silica content in thermal water component of Chiweta prospect as about 140 ppm. Assuming adiabatic (maximum steam loss) cooling and conductive cooling (no steam loss) by Fournier & Potter (1982), the subsurface temperature of Chiweta geothermal prospect was estimated to be 149°C and 157°C respectively, consistent with geothermometer estimations of Na-K and Na-K-Ca.

3.4.2 Silica-enthalpy hot spring model

Unlike chloride-enthalpy model, silica-enthalpy model handles non-boiled and boiled mixed water separately. The model assumes that no conductive cooling occurred after mixing. If the mixed water has cooled conductively, the calculated temperature of the hot water component will be too high. The other assumption is that no silica deposition has been occurred before or after mixing, and quartz controls the solubility of silica in the hot water component. The model uses quartz solubility curve and was constructed using Arnórsson (2000) equation:

$$t(°C) = -55.3 + 0.3659S - 5.3954x10^{-4}S^2 + 5.5132x10^{-7}S^3 + 74.360 \log S \qquad (4)$$

Where t is temperature in °C and S represent silica concentration in ppm. The calculated temperature is then converted to enthalpy.

This paper used H_2O ChemicaLogic SteamTab companion software (Cheng & Saini, 2003) to convert temperatures into enthalpy. The point of intersection between the data point extrapolated line and quartz solubility curve represent enthalpy of the hot water component in the mixture. Figure 9 shows Chiweta hot water component as about 660 kJ/kg corresponding to temperature of 156°C derived from steam tables.

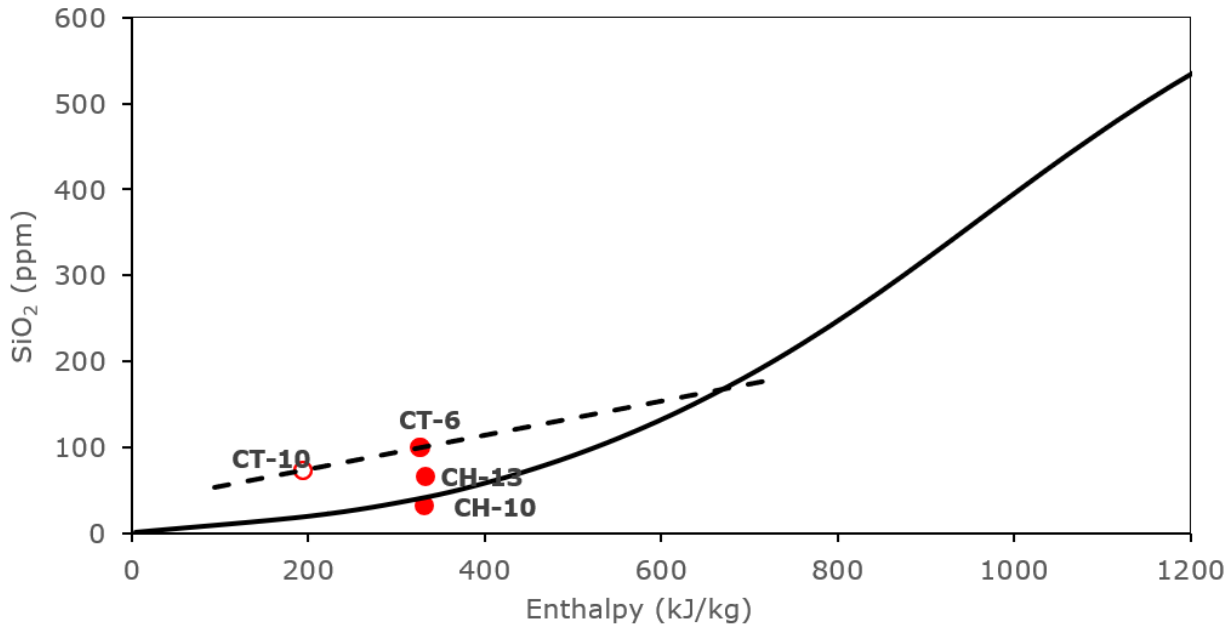

Figure 9. Silica-Enthalpy hot spring mixing model (Arnórsson, 2000) of Chiweta geothermal prospect.

The pH of 7.8 indicated that the water is gaseous and has not boiled. The extrapolated line for non-boiled water intersected the silica solubility curve meaning that the thermal springs have not cooled conductively. In this case, enthalpy changes from thermal water component (660 kJ/kg) to that of mixed water (thermal spring water, 330 kJ/kg) is due to mixing with non-thermal water of 120 kJ/kg (CT-9, 28°C). Therefore, the ratio of mixing can be obtained from silica enthalpy Figure 9 as follows:

Total thermal water enthalpy	= 660 kJ/kg (Figure 9)
Mixed water enthalpy	= 330 kJ/kg
Cold water enthalpy	= 120 kJ/kg
Enthalpy from the reservoir	= 660 kJ/kg -120 kJ/kg = 540 kJ/kg
Enthalpy of hot water in mixed water	= 330 kJ/kg - 120 kJ/kg = 210 kJ/kg
Ratio of hot water to total enthalpy	= 210 kJ/kg / 540 kJ/kg = 0.38
	= 38% parent hot water
	Therefore, cold groundwater is about 62%

The calculated ratio was used to estimate the reservoir composition of non-conservative component silica as follows:

Given:	
Measured silica (Table 1) in the mixed	= 99.43 ppm from
Hot water component in the mixed waters	= 0.38
Silica composition in the reservoir	= 99.43 ppm x 1.38
	= 137.2 ppm

The estimated silica composition of 137 ppm using silica-enthalpy mixing model was close to the composition estimated by silica-carbonate mixing model. Using geothermometer by Fournier & Potter (1982), the calculated silica reservoir composition gives subsurface temperatures of 155°C and 148°C. These subsurface temperatures were in agreement with Na-K and Na-K-Ca geothermometers displayed in Table 2.

3.4.3 The chloride-enthalpy model

The chloride-enthalpy diagram in Figure 10 was constructed using enthalpy values and chloride concentration from the water samples. The enthalpy values of data points indicated by dots (hot springs) were derived from quartz geothermometers calculated on WATCH (Bjarnason, 2010). Enthalpy values of points represented by squires (local cold waters), derived from measured temperatures. In both cases enthalpy values were calculated using H_2O ChemicaLogic SteamTab companion version 2.0 software (Cheng & Saini, 2003). The model lines in the diagram were derived using the procedure explained by Arnórsson (2000). The enthalpy of 600 kJ/kg of parent hot water corresponds to the apex of the triangle. With the aid of steam tables taking the enthalpy as that of steam saturated water, the temperature of the parent hot was estimated to be 143°C.

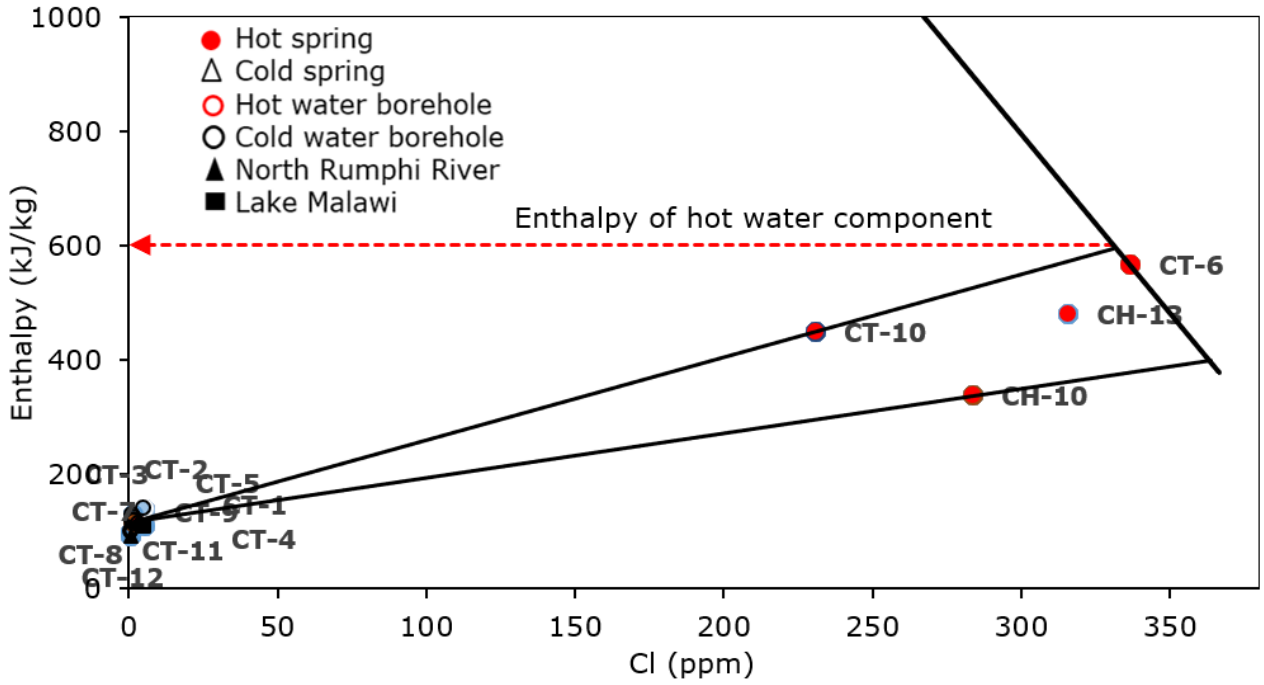

Figure 10. Chloride-enthalpy diagram (Arnórsson, 2000) for Chiweta geothermal springs.

3.5 Reconstructing reservoir water composition

Boiling, conductive cooling and mixing are very multifaceted processes and unavoidable in up-flow zone of geothermal systems (Arnórsson et al., 2007). They involve mineral dissolution and precipitation reactions. Where there is no mixing and temperatures are below 200°C, with considerable high flow rate making conductive cooling of rising fluid insignificant, aquifer fluid composition can be reasonably reconstructed below the zone of boiling. Under such conditions the boiling is assumed to be adiabatic. Studies have shown that mineral-solution equilibrium is closely approached for all major components of geothermal fluids except for Cl (Arnorsson et al., 1983; (Giggenbach, 1991). This constrains relative activities of aqueous species and also individual component concentrations and help in model validation. Cation/proton activity ratios in equilibrated liquids are constant at any specific temperature for a system of specific mineralogy. Chemical speciation programme WATCH (Bjarnason, 2010) allows to back-calculate aquifer water composition from data on the chemical composition of the boiling hot spring water. Basically, the calculation involves correction of dissolved solids content of hot spring water for the vapour loss and adding back the lost gases including CO_2 and H_2S. To run the programme a reference geothermometer temperature whether quartz, Na-K or arbitrary of aquifer is selected. The degassing coefficient (ç) needs to be selected as well. Arnórsson et al., (2007) proposed a method of selecting ç by relating it with calcite saturation. The selected ç should correspond to calcite saturation in the aquifer at selected aquifer temperature as it has been proven that geothermal reservoir water are close to calcite saturation at temperature >100°C (Arnórsson et al., 2007). The concentration of other gases apart from CO_2 and H_2S in the un-boiled aquifer is usually approximated.

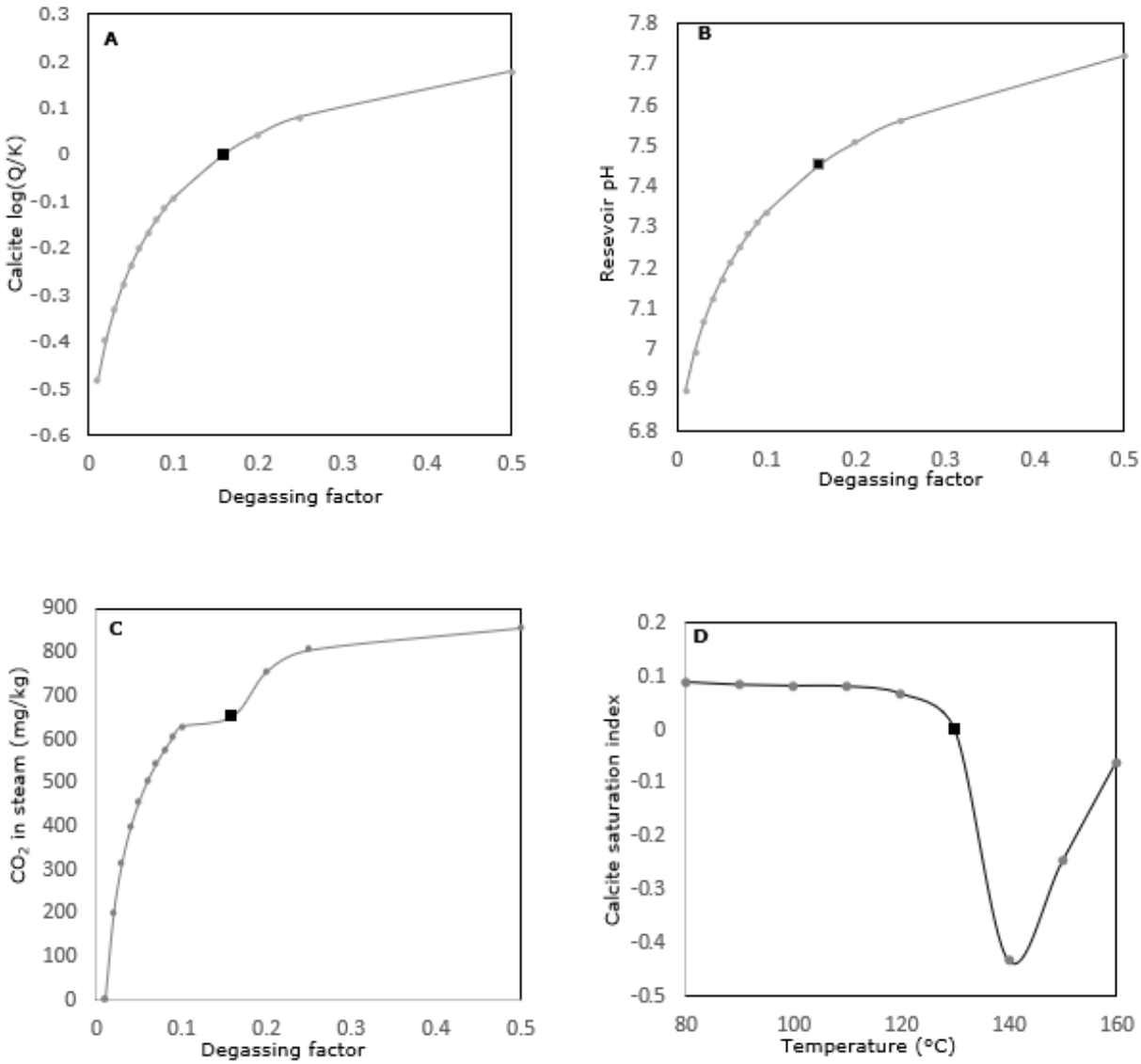

Figure 11. Modelling of aquifer (black square) and up-flow boiling of Chiweta hot spring (CH-13). A: Variation in calcite saturation in relation to CO_2 degassing of boiled water. B: pH variation in relation to degassing due to boiling. C: CO_2 steam composition against degassing of boiling water. D: Variation of calcite saturation in boiled water (adiabatic) under CO_2 degassing of 16%

Chiweta hot spring sample CT-6 and CH-13 analytical data were used for calculation of aquifer water composition. First the WATCH programme was run at different ç values taking the last temperature of last equilibrated with Na-K (149°C) as an un-boiled temperature of aquifer feeding the hot spring from depth. The first boiling was assumed to be at 100°C with 0.01 as degassing factor at about 180 m depth. Then single step adiabatic boiling was calculated in nine stages of 10°C from 160°C to hot spring temperature of 80°C. Figure 11A shows variation of calcite saturation in aquifer in relation various degassing factor (ç) values. Figure 11A shows that aquifer liquid equilibrated with calcite at ç of 0.16, indicating mild degassing. This may indicate that 16% of CO_2 in the initial aquifer liquid was transferred into vapour relative to the transfer needed to establish equilibrium distribution of CO_2 between liquid and vapour at the surface. Figure 11B illustrate that degassing of 0.16 correspond to pH of 7.45 which is close to in situ pH of 7.8. At this rate of degassing > 600 mg/kg of CO_2 escaped from the aquifer as shown in Figure 11C. This type of degassing accompanied by adiabatic cooling led to calcite saturation in Figure 11D. The temperature saturation of calcite in Figure 11D is corresponding to calculated SiO_2 geothermometer temperature of 130 °C.

Based on adiabatic boiling Arnórsson et al., (2007) developed a model for construction of reservoirs fluid composition using data from boiled hot spring at the surface. Björke et al., (2015) developed three steps for modelling reservoir fluid composition. Firstly, estimation of reservoir fluid temperature as the geothermal system is assumed to be thermodynamically isolated. In this paper the aquifer temperature of last equilibrated with Na-K (149°C) was selected. Secondly, the degree of degassing needs to be selected as well. The extent of degassing was taken from calculation in Figure 11A as 16% which correspond to calcite saturation. Thirdly, by assuming a closed system the reservoir fluid composition is given by the following equation:

$$m_i^{total} = m_i^v X^v + m_i^1 (1 - X^v) \quad (5)$$

Where m_i^{total} is the reservoir fluid composition of *i*-th composition, m_i^v and m_i^l are concentration in vapour and liquid phase respectively and X^v is the calculated vapour fraction.

For the spring, the boiling was assumed to be from the estimated reservoir temperature (149°C) to the surface temperature 80°C along water vapour saturation curve (P_{sat}). Steam fraction wass calculated using the following equation:

$$X^v = \frac{h^{fluid} - h^l}{L^l} \quad (6)$$

Where h^{fluid} is the initial fluid enthalpy obtained from the estimated reservoir temperature, h^l is the liquid enthalpy at the surface and L^l is the latent heat of vaporisation. The steam phase is $m^v = 0$ for the conservative element that do not enter into steam phase. For CO_2 and H_2S volatiles that are found in both liquid and steam phases but only analysed in liquid phase the steam phase was calculated by the following equation:

$$m_i^v = m_i^l \left(X^v \left(\frac{55.51}{P_{total} K_s \varsigma - 1} \right) + 1 \right) \quad (7)$$

where K_s is the solubility constant for a particular gas in liquid water and ς is the degassing factor. A value of unity for ς indicates equilibrium gas solubility and a value <1 present incomplete degassing or non-equilibrium degassing. WATCH software (Bjarnason, 2010) incorporate all these functions and calculate reservoir liquid composition. Table 3 shows the reservoir water composition calculated from WATCH based on data from sample CT-6 and CH-13.

Table 3: Measured chemical composition of hot spring and calculated reservoir aquifer of the Chiweta prospect. Concentration in ppm.

CT-6			**CH-13**	
	Hot spring	**Aquifer water**	**Hot spring**	**Aquifer water**
pH/°C	7.8/38.4	7.52/140	7.5	7.45/130
CO_2	59.3	51.43	28	22.85
H_2S	2.02	1.9	n.a.	
B	0.6954	0.6427	n.a.	
SiO_2	99.43	91.9	65.8	62.07
Na	383	353.98	389.2	367.11
K	23.2	21.44	21.3	20.09
Mg	0.387	0.358	0.419	0.395
Ca	17.96	16.6	17.23	16.25
F	12.63	11.673	12.82	12.092
Cl	336.7	311.19	316	298.06
SO_4	295.7	273.29	287.3	270.99
Al	0.0114	0.0105	n.a.	
Fe	n.d.		n.a.	
TDS Vapour phase	n.a.		1300	1226.22
CO_2	n.a.	1285.65	n.a.	754.93
H_2S	n.a.	10.91	n.a.	

The reconstructed reservoir water belongs to Na-Cl-SO_4-HCO_3 facies. Table 3 displays re-calculated reservoir composition with lower concentrations than in situ. This may be explained by phase separation of the aquifer water as it ascends to the sampling point. As explained by D'Amore & Arnórsson (2000) that cooling bring modification in the chemical composition of the ascending fluid by phase separation of steam and liquid water phases giving rise to an increase of non-volatile components in the discharged hot spring water. Though concentration changed, the calculated reservoir composition gave Na-Cl type similar to the water discharged

from the hot springs. The reservoir pH is slightly low compared to the in situ due to loss of CO_2 to the atmosphere leaving the spring water more basic.

3.6 Determining origin of water using isotopes and mobile elements

Deuterium, boron and chloride are natural tracers that have been used to establish origin of water in geothermal fields. Giggenbach (1991) defined them as non-reactive (chemically inert) constituency in natural waters that remained unchanged and act as a tag for mapping movement of water. In this paper these three tracers were used to determine the original component of geothermal water and to assess water rock-interaction process.

Isotopes are expressed as a ratio of heavy isotope (rare) against light (abundant) isotope. For oxygen and hydrogen isotopes, the concentration is written with reference to international a standard known as standard mean oceanic water (SMOW). For example, oxygen isotopes are expressed as follows;

$$\delta(^{18}O/^{16}O) = \frac{(^{18}O/^{16}O)_{sample} - (^{18}O/^{16}O)_{SMOW}}{(^{18}O/^{16}O)_{SMOW}} x1000 \quad (8)$$

Stable isotopes especially δD and $\delta^{18}O$ has become essential component in geothermal investigation. Similar to other isotopes, δD and $\delta^{18}O$ ratios are sensitive to changes in temperature, water-rock interaction and other physicochemical processes such as mixing and steam separation (Arnórsson, 2000) as ion exchange reactions in the natural system achieve equilibrium depending on temperature. Isotopes fractionate in the chemical processes responding to natural systems. The fractionation is greatest in lighter element such as hydrogen and oxygen. The δD and $\delta^{18}O$ isotopes are suitable tracer of the origin of water and its flow direction as it have ability to retain its physical and chemical characteristics (Arnórsson, 2000; Sharp, 2007). As such, δD and $\delta^{18}O$ has been used to define hydrogeological conditions and evaluate the processes that have affect the fluid. This due to the fact that δD and $\delta^{18}O$ isotopes ratio have little change over a long distance. Deuterium (δD) is one of the three hydrogen isotopes (protium, deuterium and tritium) containing one neutron and a proton within its nucleus with atomic mass of 2 atomic mass unit (amu) (Sharp, 2007).

Table 1 shows the deuterium (δD) and oxygen ($\delta^{18}O$) isotope values of Chiweta geothermal waters obtained from ICP-MS. Craig (1963) and White (1986) established that originate of most geothermal water is mainly meteoric therefore the data was compared to global meteoric water line. The globe precipitation line (GML) in Figure 12 shows the relationship of δD and $\delta^{18}O$ isotopic values of geothermal water, cold groundwater and surface waters (Lake Malawi and North Rumphi River) in Chiweta area. It was observed that geothermal water and groundwater (δD=-30.61 to -18.87‰, $\delta^{18}O$= -5.4 to -3.07‰) follow closely to global meteoric water line ($\delta D=8\delta^{18}O+10$) demonstrating meteoric origin of both waters. Also noted was very slight shift of $\delta^{18}O$ in thermal water (CT-6= -4.08‰ and CT-10=-3.56‰) and groundwater (CT-2= -3.07‰) which can be attributed to progressive water-rock interaction.

Lake Malawi water was enriched in heavy δD and $\delta^{18}O$ (δD=12.49 -15.06‰ and $\delta^{18}O$=1.67-2.27‰) compared to the groundwater (δD=-30.61 to -18.87‰, $\delta^{18}O$= -5.4 to -3.07‰) as demonstrated by the shift away from GML in same Figure 12. The explanation to that behaviour was that, the lake was very much exposed to evaporation. Vapour pressure of lighter isotope ($H_2{}^{16}O$) is higher than vapour pressure of both heavier ones (HDO and $H_2{}^{18}O$). As such, evaporation takes lighter δH and ^{16}O isotopes into the lake water vapour phase leaving heavy isotopes in liquid phase of the lake water. Therefore, remaining lake water is enriched in heavier HDO and $H_2{}^{18}O$. North Rumphi water showed relatively more depleted in heavy isotopes (δD= -34.04 to -33.94‰ and $\delta^{18}O$ = -6.50 to -4.96‰) compared to rest of the samples. This may be explained by different source of river water than groundwater, probably originated as precipitation farther western highlands on high altitude.

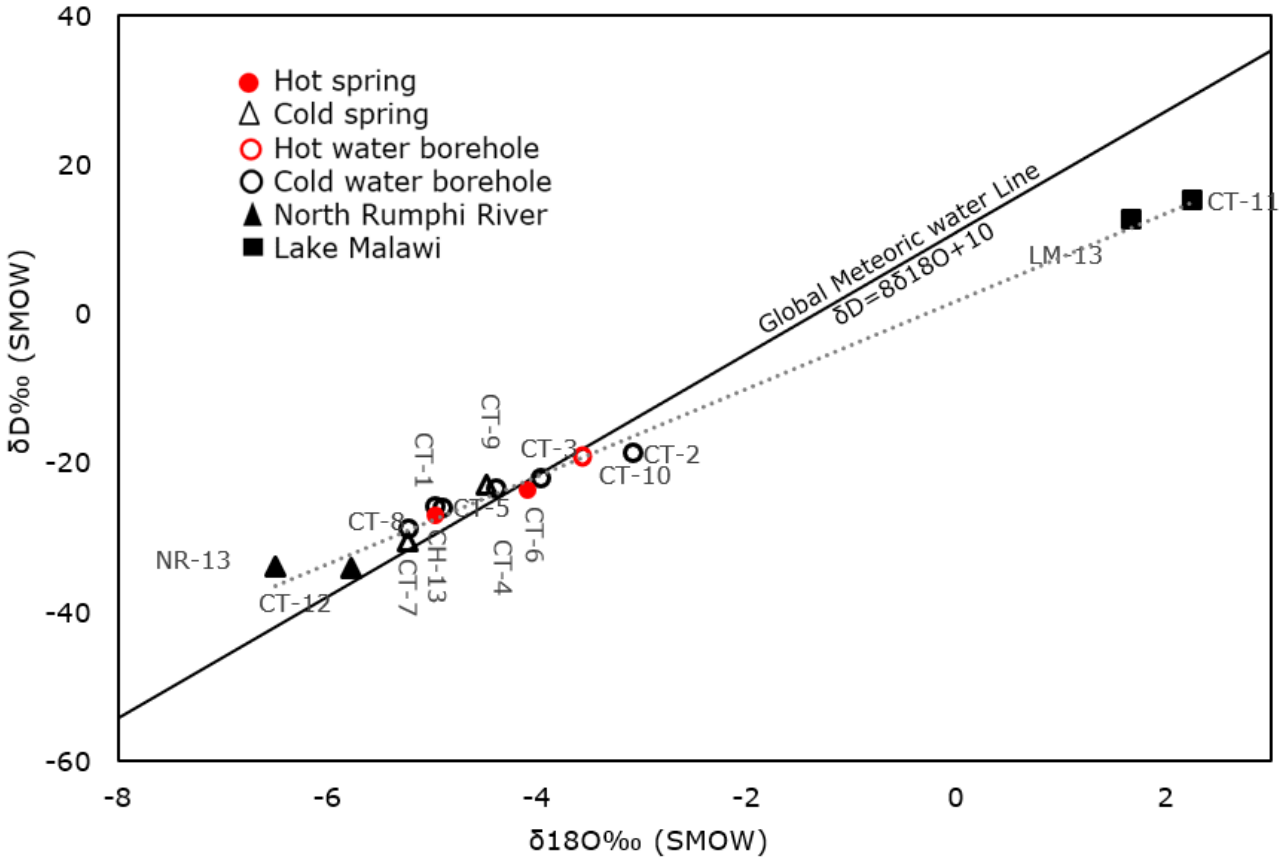

Figure 12. The relationship between isotopes (δD and $\delta^{18}O$) of Chiweta sampled waters and Globe Meteoric Line (GML)(Arnórsson, 2000).

3.7 Water-rock interaction

Apart from water-rock interaction, other processes also affect isotopic fractionation. Therefore, before considering water-rock interaction process, isotopic data obtained from boiled or close to boiled hot spring need to calculated to reservoir conditions to account for effect of isotopic changes due to boiling and phase separation (D'Amore & Arnórsson, 2000). Isotopic investigations has ability to quantify processes occurred in geothermal system such as boiling, steam separation and condensation. As geothermal water ascend to the surface physical processes and chemical changes brought about by conduction, mixing and boiling are replicated in both chemical and isotopic component of the fluid (D'Amore & Arnórsson, 2000). According to steam separation mechanism, phases of steam separation has different effects on isotopic fractionation (D'Amore & Arnórsson, 2000). One stage separation yield maximum isotopic fractionation than multi-stage which resulted into minimum isotopic fractionation. Boiling leads to fractionation of deuterium and ^{18}O through enrichment of the heavier isotopes in water phase consistent with depletion of the same in the steam phase.

The $\delta^{18}O$ of geothermal water usually displaced from meteoric line towards higher values (less negative) due to exchange of ^{18}O between water and rock (Arnórsson, 2000). The extent of the shift is proportional to degree of water-rock interaction. Which follows that the more the water -rock interaction the higher the shift. Increase in temperature enhances chemical reaction including water-rock interaction which in turn intensifies $\delta^{18}O$ shift (D'Amore & Arnórsson, 2000). In case of Chiweta the shift is very minimal which may be possibly caused by limited water-rock interaction.

In this paper the assessment of isotopic reservoir condition was done using the method proposed by D'Amore & Arnórsson, (2000). By assuming one stage adiabatic boiling to attain maximum fractionation from quartz and Na-K geothermometer of 140 °C to temperature of 100 °C, isotope composition of the aquifer was calculated. The first step involved calculation steam fraction using the following equation:

$$Y_{100} = \frac{h^d - h^w_{100}}{L_{100}} \tag{9}$$

Where Y_{100} is the steam fraction formed by the boiling from reservoir temperature to 100 °C whereas h^d and h^w_{100} represent the enthalpy of the aquifer water and the steam saturated water at 100 °C respectively. L_{100} is the latent heat of vaporization at 100 °C. Using steam table (Cheng & Saini, 2003), the aquifer temperatures and 100 °C temperature were converted to enthalpy and steam fraction was calculated using equation (9) above as follows:

$$Y_{100} = \frac{589 - 419}{2257} = 0.0753 \tag{10}$$

Conservation mass of isotopes was given by the following equation:

$$\delta_d = \delta_{A,C}(1 - Y_C) + \delta_{B,C}Y_C \quad (11)$$

Where δ_d is isotopic value in the reservoir water and $\delta_{A,C}$ and $\delta_{B,C}$ are its δ values in two phase respectively at 100 °C.

The second step was determination of fractionation factor between two phases using the following equation:

$$10^3 In\alpha_{A-B} = \delta_A - \delta_B \quad (12)$$

The fractionation factor for ^{2}H and ^{18}O between water and steam from Truesdell, Nathenson, & Rye (1977) as reported by D'Amore & Arnórsson (2000) are 5.24 and 27.8 respectively. From equation (12) the fractionation factors can be written as;

$$10^3 In\ \alpha\ (^2H) = \delta(^2H)_l - \delta(^2H_v) = 27.8 \quad (13)$$

$$10^3 In\ \alpha\ (^{18}O) = \delta(^{18}O)_l - \delta(^{18}O_v) = 5.24 \quad (14)$$

Combination of equation (11) and equation (12) and elimination of δ_B resulted in formulation of the following equation

$$(\delta^2H)_d\ = (\delta^2H)_{w,c} - Y_C.10^3\ In\ \alpha(^2H)_{(w-S),c} \quad (15)$$

$$(\delta^{18}O)_d\ = (\delta^{18}O)_{w,c} - Y_C.10^3\ In\ \alpha(^{18}O)_{(w-S),c} \quad (16)$$

For sample CT-6 the reservoir isotope values were

$$(\delta^2H)_d = -23.77 - 0.0753\text{x}27.8 = -25.86$$

$$(\delta^{18}O)_d = -4.08 - 0.0753\text{x}5.24 = -4.47$$

Table 4: Calculated isotope reservoir composition based on equations (15) and (16)

	Sample		**Reservoir**	
Name	δD	δ^{18}O	δD	δ^{18}O
CT-6	-23.77	-4.08	-25.86	-4.47
CH-13	-26.0	-4.96	-28.11	-5.35
CT-10	-19.19	-3.56	-21.28	-3.96

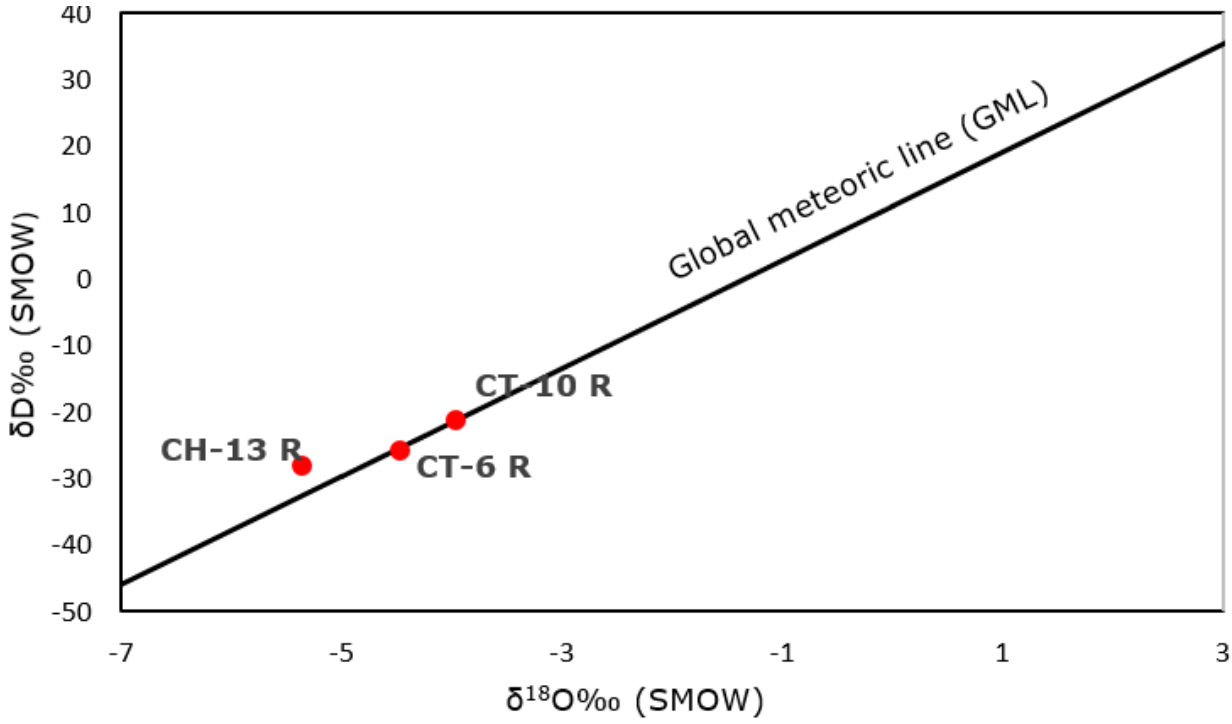

Figure 13. The relationship between calculated reservoir water isotopes (δD and $\delta^{18}O$) values for Chiweta area (dots) and Globe Meteoric Line (GML) from Arnórsson (2000)

Figure 13 shows the relationship of δD and $\delta^{18}O$ isotopic values of calculated reservoir geothermal water (Table 4) and global meteoric line. The reservoir water CT-6 and CT-10 plotted on global meteoric water line ($\delta D=8\delta^{18}O+10$) demonstrating total meteoric component. Its only sample CH-13 which plotted further left of the meteoric line. All samples showed the same behavior of shifting left (becoming more negative) comparing to hot spring isotopic values plots in Figure 12 . This characteristic may not be interpreted as due water-rock interaction in the reservoir. Other processes such as phase segregation might be responsible for such behavior.

3.8 Discussion

The low EC in surface water reflecting low water-rock interaction but O_2 consumption of decaying organic matter typically shows a HCO_3 alkaline-earth composition. The low concentration of chloride implies low salinity reflecting predominance of meteoric contribution supported by HCO_3 being the main anion. Substantial acidic in cold groundwater denote meteoric component with relatively shallow and fast underground circulation within the aquifer. This is supported by previous study (Wanda et al., 2013) which found groundwater enriched with soil CO_2. The low concentration of silica in lake water suggested precipitation or consumption of silica forming organisms or chert formation. Substantial shift of lake water δD and $\delta^{18}O$ from global meteoric line to more positive values signify high isotopic fractionation due to high rate of evaluation in the lake. The North Rumphi River water showed lower $\delta^{18}O$ and δD values (more negative) than groundwater meaning that the river water originated as precipitation from farther away from western highlands on high altitude. According to water classification (Ellis & Mahon, 1977; Giggenbach, 1991; White, 1986) the surface and groundwater of the Chiweta area is categorized as bicarbonates water of meteoric origin.

Silica was the major continuant in the Chiweta hot spring waters together with sodium being major cation. Sulphate was dominant anion seconded by chloride and bicarbonate. The relative abundant of chloride in geothermal water means increased salinity (Arnórsson, 1995a). Using Ellis & Mahon, (1977); Giggenbach (1991); and White (1986) methods of water classification geothermal water of Chiweta is referred as sodium-chloride water with small bicarbonate component. Similar water type was also reported by Kemp (1975) as the main type the Chiweta.

The neutral pH of geothermal water denotes meteoric origin but with slightly modified pH compared to surface and cold groundwater due to deeper circulation. The origin of geothermal waters was the groundwater from local rain other than the lake water as verified by close similarities in δD and $\delta^{18}O$ values between groundwater and geothermal water. The differences in isotopic values between geothermal water and lake water indicate that the origin of geothermal water is not the lake. The higher EC in hot spring water reflect relatively more water-rock interaction as the result of deeper and long circulation path. However, the interaction is not high enough to cause isotopic fractionation. No boiling has been registered in the up-flow zone as demonstrated by silica-carbonated mixing model.

Isotopic studies of thermal water and non-thermal water showed that $\delta^{18}O$ and δD values of groundwater and calculated geothermal reservoir water plotted on global meteoric line whereas hot spring water showed slightly higher values (less negative). This indicates that both the groundwater and geothermal water were from local precipitation but spring thermal water deuterium and oxygen isotopes fractionated. Loss of steam might be responsible increased concentration and isotopic fractionation of the hot spring water compared to reservoir water.

Chiweta geothermal prospect is suggested to fall within low temperature geothermal system bracket (Saemundsson, Axelsson, & Steingrímsson, 2009) as verified by the estimated reservoir temperature of 132-157 °C using solute geothermometers (Arnorsson et

al., 1983; Fournier & Potter, 1982; Fournier & Truesdell, 1973; Truesdell, 1975). Multiple mineral equilibrium estimated subsurface temperature within the same range 130-140°C of silica and Na-K geothermometers. Mixing models (Arnórsson, 2000; Fournier & Potter, 1982) subsurface temperature estimation is in agreement with cation geothermometers (Arnorsson et al., 1983; Fournier & Truesdell, 1973; Truesdell, 1975). The geothermal system is located within elevated geothermal gradient geological setting. The low temperature Chiweta can further categorized as sedimentary geothermal system type as demonstrated by circulation of water through NW-SE and NE-SW trending faults into the tectonically lifted hot sedimentary and metamorphic rocks.

3.8.1 Model

Both thermal and non-thermal waters of Chiweta prospect represent the local precipitation fallen in the southwest, western and northwest close highlands. Driven by hydraulic gradient at an elevation above1200 m, the recharging Ca-Mg-HCO_3 groundwater originate from the highlands at temperatures of around 23 to 33°C and pH of 5.7-7.5. These waters percolate underground through faults and fractures of NW-SE and NE-SW trending that sliced Karroo sedimentary beds and metamorphosed basement rock as verified by both hydro-geological analysis of the flow direction, δD and $\delta^{18}O$ stable isotopes. The inflow waters are considered to attain the heat from increased geothermal gradient at depth. The heat source might be the hot rocks in the roots of the geothermal system (Arnórsson, 1995a).

The estimated subsurface temperature based on quartz, Na-K and Na-K-Ca geothermometers indicated subsurface temperature of about 132 to 157°C. Multiple mineral equilibria temperature estimation showed similar range of temperatures despite some deviation. Silica-carbonate, silica enthalpy and chloride enthalpy mixing models also supported the estimated geothermometers.

Assessment of saturation indices, activity coefficients of the sample above 100°C take into account the reconstructed reservoir composition. The saturation indices for both hot spring water sample CT-6 and CH-13 from the study area give negative values for anhydrite. Calcite and quartz are saturated in both hot spring water. However the saturation is low to cause scaling problems. Talc and chrysotile, quartz and calcite saturation are high in the recalculated reservoir composition. Therefore, possibilities of deposition of such minerals are high.

As temperature increases due to increased geothermal gradient, water-rock interaction progresses, dissolving some mineral from the rock into aqueous phase. This in turn changes the initial composition of Ca-Mg-HCO_3 water to Na-Cl type. The increase in temperature and change in chemical composition by water-rock interaction has minimal effect the isotopic composition of thermal water as witnessed by calculated δD and $\delta^{18}O$ isotope composition of thermal water slight negative shift and plotted on the global meteoric line.

The upward movement of water to the out-flow zone is convectively driven due to different in density of the hot and cold water columns within and outside the geothermal system respectively. This density difference create enough pressure difference to sustain the water convection (Arnórsson, 1995b).

There is no boiling in the upflow zone as demonstrated by silica-carbonate mixing model. As such, degassing at the surface is only suggested possible process affecting the isotope fractionation by allowing depleted vapour escape from thermal water, leaving the hot spring water relatively enriched in heavier δD and $\delta^{18}O$ isotopes compared to reservoir water. Silica-enthalpy mixing model showed mixing of 62% of shallow groundwater with geothermal water in the upflow zone contributing to dilution of the thermal spring waters.

At the surface Chiweta geothermal system is manifested by linear cluster of hot springs. The estimated total flow rate of the springs is about 30 L/s producing nonreactive alkaline water which favours growth of ague and other surrounding vegetation. No silica sinter was deposited around the hot springs. However, miner silica and sulphur deposits were noticed with odor of sulphur smell.

4. CONCLUSION

Careful and thoughtful use of hydrogeochemistry techniques has acquired very useful information on the resource temperature, process reservoir and up-flow processes, its chemistry and potential problems likely to affect exploitation of the resource.

The origin of recharge water is from the local precipitation fallen in the southwest, western and northwest close highlands. This Ca-Mg-HCO_3 water type is driven by hydraulic gradient from an elevation above1200 m. These waters percolate underground through faults and fractures of NW-SE and NE-SW orientation. There is no lake water feeding the geothermal system.

Geochemistry investigations demonstrated that the Chiweta is a low temperature geothermal system with reservoir temperature of about 132-157 °C based on quartz (Fournier, 1977), Na-K, (Arnorsson et al., 1983) and Na-K-Ca cation geothermometers supported by multiple mineral equilibria and mixing models. This elevated temperature is enough to drive minimal water rock interaction leading to increase of minimal stable isotopic fractionation.

Thermal spring waters are undersaturated with respect to anhydrite. The same hot spring waters are mild saturated with regard to calcite and quartz. This indicates minimal chances of scaling problems. There are high chances of talc and chrysotile, quartz and calcite deposition from recalculated reservoir composition due their high saturation.

Stable isotopes in thermal water suggested fractionation due to phase separation at the surface, without boiling according to silica-carbonate mixing model. However mixing of shallow groundwater and geothermal was noted according to silica-enthalpy mixing model and chloride-boron plots. Thermal water from the boreholes had higher proportion of cold groundwater than hot spring water. At the surface thermal water have temperatures between 60-80°C and are mostly Na-Cl-SO4-HCO3 type with SiO_2 content ranging from 31 to 99 ppm.

REFERENCES

Ármannsson, H., & Ólafsson, M. (2006). Collection of geothermal fluids for chemical analysis. Iceland Geosurvey.

Arnórsson, S. (1995a). Geothermal systems in Iceland: Structure and conceptual models-I. High-temperature areas. Geothermics, 24(5–6), 561–602.

Arnórsson, S. (1995b). Geothermal systems in Iceland: Structure and conceptual models-II. Low-temperature areas. Geothermics, 24(5–6), 603–629.

Arnórsson, S. (2000). Isotopic and chemical techniques in geothermal exploration, development and use. International Atomic Energy Agency, 109–111.

Arnórsson, S., & Andrésdóttir, A. (1995). Processes controlling the distribution of boron and chlorine in natural waters in Iceland. Geochimica et Cosmochimica Acta, 59(20), 4125–4146.

Arnórsson, S., Bjarnason, J. Ö., Giroud, N., Gunnarsson, I., & Stefánsson, A. (2006). Sampling and analysis of geothermal fluids. Geofluids, 6(3), 203–216.

Arnorsson, S., Gunnlaugsson, E., & Svavarsson, H. (1983). The chemistry of geothermal waters in Iceland. III. Chemical geothermometry in geothermal investigations. Geochimica et Cosmochimica Acta, 47(3), 567–577.

Arnórsson, S., Stefánsson, A., & Bjarnason, J. Ö. (2007). Fluid-fluid interactions in geothermal systems. Reviews in Mineralogy and Geochemistry, 65(1), 259–312.

Bjarnason, J. Ö. (2010). The chemical speciation program WATCH, version 2.4 (Version 2.4). Reykjavik, Iceland.: ISOR – Iceland GeoSurvey.

Björke, J. K., Stefánsson, A., & Arnórsson, S. (2015). Surface water chemistry at Torfajökull, Iceland—Quantification of boiling, mixing, oxidation and water–rock interaction and reconstruction of reservoir fluid composition. Geothermics, 58, 75–86.

Cheng, G. C., & Saini, R. (2003). ChemicaLogic SteamTab companion Version 2.0 (Version 2.0). Burlington, USA: ChemicaLogic Corporation.

Chorowicz, J. (2005). The East African rift system. Journal of African Earth Sciences, 43(1), 379–410.

Chorowicz, J., & Sorlien. (1992). Oblique extensional tectonics in the Malawi Rift, Africa. Geological Society of America Bulletin, 104(8), 1015–1023.

Climate Data. (2017). Climate Chiweta: Temperature, Climate graph, Climate table for Chiweta - Climate-Data.org. Retrieved 24 May 2017, from https://en.climate-data.org/location/207402/

Craig, H. (1963). The isotopic geochemistry of water and carbon in geothermal areas. Nuclear Geology on Geothermal Areas, 17–53.

D'Amore, F., & Arnórsson, S. (2000). Geothermometry.

Dulanya, Z., Morales-Simfors, N., & Sivertun, Å. (2010). Comparative study of the silica and cation geothermometry of the Malawi hot springs: Potential alternative energy source. Journal of African Earth Sciences, 57(4), 321–327.

Ellis, A. J., & Mahon, W. A. J. (1977). Chemistry and geothermal systems. Academic Press.

Flannery, J. W., & Rosendahl, B. R. (1990). The seismic stratigraphy of Lake Malawi, Africa: implications for interpreting geological processes in lacustrine rifts. Journal of African Earth Sciences (and the Middle East), 10(3), 519–548.

Fontijn, K., Williamson, D., Mbede, E., & Ernst, G. G. (2012). The Rungwe Volcanic Province, Tanzania–A volcanological review. Journal of African Earth Sciences, 63, 12–31.

Fournier, R. O. (1977). Chemical geothermometers and mixing models for geothermal systems. Geothermics, 5(1–4), 41–50.

Fournier, R. O., & Potter, R. W. (1982). Revised and expanded silica (quartz) geothermometer. Bull., Geotherm. Resour. Counc.(Davis, Calif.);(United States), 11(10).

Fournier, R. O., & Truesdell, A. H. (1973). An empirical Na-K Ca geothermometer for natural waters. Geochimica et Cosmochimica Acta, 37(5), 1255–1275.

Geological Survey Department. (2010). Report on geological and structural mapping of the karonga earthquakes affected areas (p. 19). Zomba, Malawi: Ministry of Natural Resources, Energy and Environment. Unpublished report

Geothermal Development Company. (2010). Assessment of the geothermal potential of Malawi. Nairobi Kenya: GDC. Unpublished report

Giggenbach, W. F. (1986). Graphical techniques for the evaluation of water–rock equilibration conditions by use of Na, K, Mg and Ca contents of discharge waters. In Proc. 8th New Zealand Geothermal Workshop (pp. 37–44).

Giggenbach, W. F. (1988). Geothermal solute equilibria. Derivation of Na-K-Mg-Ca geoindicators. Geochimica et Cosmochimica Acta, 52(12), 2749–2765.

Giggenbach, W. F. (1991). Chemical techniques in geothermal exploration. Application of Geochemistry in Geothermal Reservoir Development, 11, 9–144.

Harrison, D. R., & Chapusa, F. W. P. (1975). The geology of the Nkhotakota-Benga Area (Bulletin No. 32) (p. 33). Zomba, Malawi: Geological Survey Department.

Kemp, J. (1975). The geology of the Uzumara area. Government Printer, Zomba Malawi.

Mdala, H. (2015, February). Dertemination of structural variations between northern and southern pronvinces of Malawi rift by using of automatic lineament extraction methods. University of Twente.

Powell, T., & Cumming, W. (2010). Spreadsheets for geothermal water and gas geochemistry. In Proceedings.

Ray, G. E. (1975). The geology of the Chitipa-Karonga area (Bulletin No. 42) (p. 33). Zomba, Malawi: Geological Survey Department.

Reed, M., & Spycher, N. (1984). Calculation of pH and mineral equilibria in hydrothermal waters with application to geothermometry and studies of boiling and dilution. Geochimica et Cosmochimica Acta, 48(7), 1479–1492.

Ring, U. (1995). Tectonic and lithological constraints on the evolution of the Karoo graben of northern Malawi (East Africa). Geologische Rundschau, 84(3), 607–625.

Saemundsson, K., Axelsson, G., & Steingrímsson, B. (2009). Geothermal systems in global perspective. Short Course IV on Exploration for Geothermal Resources, 1–22.

Saria, E., Calais, E., Stamps, D. S., Delvaux, D., & Hartnady, C. J. H. (2014). Present-day kinematics of the East African Rift. Journal of Geophysical Research: Solid Earth, 119(4), 3584–3600.

Sharp, Z. (2007). Principles of stable isotope geochemistry. Pearson education Upper Saddle River, NJ.

Thatcher, E. C. (1974). The geology of the Nyika area. Government Printer, South Africa.

Truesdell, A. H. (1975). Summary of section III geochemical techniques in exploration. In Proceedings, Second UN Symp. on the Development and Use of Geothermal Resources, San Francisco (Vol. 1).

Truesdell, A. H., Nathenson, M., & Rye, R. O. (1977). The effects of subsurface boiling and dilution on the isotopic compositions of Yellowstone thermal waters. Journal of Geophysical Research, 82(26), 3694–3704.

Wanda, E. M., Gulula, L. C., & Phiri, A. (2013). Hydrochemical assessment of groundwater used for irrigation in Rumphi and Karonga districts, Northern Malawi. Physics and Chemistry of the Earth, Parts A/B/C, 66, 51–59.

White, D. (1986). Subsurface waters of different origins. In Fifth international symposium on water-rock interaction. Extended abstracts. Inernational Association of Geochemistry and Cosmochemistry, Orkustofnun, Reykjavík (pp. 629–632).